Synthesis of (-)-drimenol as potential antifungal agent and synthesis of chiral substituted polyvinylpyrrolidones

by

Edruce Edouarzin

A.S., Bronx Community College, City University of New York, 2014
B.S., Lehman College, City University of New York, 2019

A THESIS

submitted in partial fulfillment of the requirements for the degree

MASTER OF SCIENCE

Department of Chemistry
College of Arts and Sciences

KANSAS STATE UNIVERSITY
Manhattan, Kansas

2022

Approved by:

Major Professor
Dr. Duy H. Hua

Copyright

Abstract

The success of modern medicine to cure and treat ailments is contributed to the ability to properly diagnose the cause of the symptoms. Fungal diseases are underestimated and often disregarded as a potential public health risk. The misdiagnosis of ailments either caused or exacerbated by fungal pathogens can endanger many lives. Fungal strains such as *C. auris* and *C. haemulonii* exhibit resistance to many commonly used fungicides, suggesting a need for alternative means of treatment. (-)-Drimenol has been found to work well at inhibiting the growth of *C. albicans* at concentrations as low as 8 μg/ml and tolerable by *Caenorhabditis elegans* (roundworms) at 100 μg/ml. In this thesis I discuss the inspiration and synthesis of drimenol and analyze its potential as an antifungal agent.

Catalysis is the backbone of many industrial processes and reactions. Asymmetric oxidations have been explored but there are still many shortcomings in terms of enantioselectivity. Poly-N-vinylpyrrolidinone (PVP) is an efficient stabilizer for nanoclusters and has been found to regulate aggregation of the metal atoms. Some researchers have reported increased reactivity by these supported clusters, but enantioselective oxidations were still a challenge. The Hua lab previously reported their success in performing stereo- and regioselective oxidations on various alkenes and cyclic alkanes using C5-substituted PVPs stabilized Pd/Au and Cu/Au bimetallic nanoclusters, respectively. In this thesis, I describe the synthesis of a second generation C3-substituted PVP to determine how the alternate substitution may affect the enantioselectivity.

Table of Contents

List of Figures……..v

Acknowledgements……vi

Chapter 1 - Synthesis and Characterization of (-)-Drimenol……...1

1.1. Introduction……...1

1.2. Discovery and Risks of *C. Auris*……..….1

1.3 Drimane Sesquiterpenoids as Potential Antifungal Agents……...2

1.4 Synthesis of (-)-Drimenol and Analogues……...……..……3

1.5 Results……5

1.6 Experimental Procedure…….....7

Chapter 2 - Synthesis and Characterization of Chiral Substituted Polyvinylpyrrolidones..... 13

2.1. Introduction……13

2.2. Effects of Bimetallic Nanoclusters……13

2.3 Poly(*N*-vinyl-2-pyrrolidone) Supported Nanoclusters…….……14

2.4 Discussion……16

2.5 Conclusion……...18

2.6 Experimental Procedure……...19

References..... 27

Appendix A – ^{1}H and ^{13}C NMR spectra of synthesized molecules..... 30

List of Figures

Figure 1. Effect of drimenol and fluconazole on *C. auris* growth. 6
Figure 2. Drimenol tolerance test with *Caenorhabditis elegans*. 7
Figure 3. Proposed mechanism for the activation of molecular oxygen by Au:PVP. 15
Figure 4. Representative asymmetric oxidations previously reported by Hua et al., 2016. 16

Acknowledgements

I would like to thank my advisor Dr. Hua for his support and continued guidance. It has been an honor to work in his laboratory and learn directly from such a brilliant mind. My first time working in his laboratory was as a participant in the NSF Research Experience for Undergraduates (REU) program. That experience made higher education seem more attainable than I had previously imagined. As a first generation American and first in my family to pursue a graduate degree, I felt a lot of pressure to meet the expectations of my family, friends, and community. There were times where I would feel so overwhelmed by these thoughts that it impaired my ability to focus but Dr. Hua's patience and continued support helped me regain perspective. I learned various useful laboratory skills and techniques that will serve as tools to help me succeed as I enter this new phase in my life, and I could not be more thankful.

I would also like to thank my graduate committee members Dr. Ping Li, Dr. Jun Li, and Dr. Yong Cheng Shi for their support and suggestions during my three-semester review and graduate experience. As well as the other faculty and staff members of the chemistry department that provided guidance, helped expand my knowledge of the field, and aided in maintaining laboratory equipment.

I want to thank my laboratory members Zongbo Tong and Zhaoyang Ren for always being available and helping with tasks around the laboratory. I also want to thank the postdoctoral fellows I have had the honor of working beside such as Dr. Huafang Fan, Dr. Shunya Morita, Dr. Kanchan Mishra, Dr. Lingaraju Gorla, and Dr. Deepak Barange for imparting some of their wisdom on to me. I want to thank the friends I made here in Kansas for serving as my support system away from home, as well as the support system I have back home. Lastly, I want to thank my parents for making the sacrifices they did so that I could have made it into graduate.

Chapter 1 - Synthesis and Characterization of (-)-Drimenol

1.1. Introduction

Fungal diseases are often neglected as a public health issue. Most fungal infections are caused by contacting fungi that are commonly found in the environment. Although there are many harmless fungal infections, there are some that pose a significant risk to people with weakened immune systems. This includes people living with autoimmune diseases such as HIV, organ transplant recipients, cancer patients, and premature neonates. The UNAIDS organization reported that 1.5 million people acquired HIV, and 37.7 million were currently living with it as of 2020 alone[1]. In addition, mechanically ventilated COVID-19 patients have been found to be at risk of SARS-CoV-2-associated pulmonary aspergillosis (CAPA)[2]. As the number of immunocompromised people increase, so does the risk of falling victim to a fungal disease.

1.2 Discovery and Risks of *Candida Auris*

Candida auris was first reported in 2009, after being isolated from the discharge from the external ear cavity of a 70-year-old patient at Tokyo Metropolitan Geriatric Hospital in Tokyo, Japan[3]. Prior to the identification of *C. auris*, 8 cases of fungemia (blood infection caused by fungi) and 15 cases of chronic otitis media (ear infection) from 5 separate hospitals in Korea between 2004-2006[4]. Researchers originally identified it as the phenotypically similar *C. haemulonii*, which was rarely seen to cause such invasive infections. The two strains are so similar that molecular methods are required to differentiate them, but that may prove difficult for facilities with limited resources. In addition, *C. haemulonii* was found to have resistance to the antifungal agents amphotericin B, itraconazole and fluconazole by prior studies, after an outbreak was observed among neonates[5]. In 2015, the US Centers for Disease Control (CDC)

assisted with an outbreak of bloodstream infections (BSIs) and positive urine cultures at a hospital in Pakistan[6]. The origin of the infections was presumed to be caused by *Saccharomyces* but were later identified as *C. auris*, which had not yet been previously reported by Pakistani institutions. The CDC investigated similar incidents around the world and found cases in several countries such as Venezuela, India, South Africa, and Kuwait[7–10]. Alarmingly, a substantial number of cases seemed to originate from hospital settings[6]. This led to an increased interest in understanding the epidemiology and extent of drug resistance of *C. auris*. Improper identification of the strains and limited access to alternate antifungal agents will greatly limit the ability for institutions to properly treat these infections.

1.3 Drimane Sesquiterpenoids as Potential Antifungal Agents

In an attempt to find an alternative drug to combat drug resistance in tuberculosis, researchers turned their attention to the plant *Warburgia salutaris*[11]. *W. salutaris* is a flowering tree native to South Africa that was traditionally used to treat the symptoms of chest and respiratory infections. To this effect, the crude extract from the bark and purified isolated compounds were investigated for their effect on mycobacterial growth, ultra-structural cell morphology, and on the activity of pure recombinant mycobacterial arylamine N-acetyltransferase (NAT). The NATs of *Mycobacterium tuberculosis* and *Mycobacterium bovis*, the causative agents in tuberculosis, were investigated, and isoniazid was found to activate NAT. Isoniazid was formerly used to treat the virus[12]. An overall increased expression of NAT in *M. tuberculosis* and other bacteria was found to cause an increased resistance to INH and other arylamine-based drugs. The crude extract was found to inhibit the growth of *M. tuberculosis* and the acetylation process, and the partially purified crude was found to impair the outer cell wall structure of *M. bovis*[11]. The major

component isolated from the extract was 11α-hydroxycinnamosmolide, which was degraded to cinnamodial by the liquid chromatography-mass spectroscopy (LC-MS) process during characterization. 11α-Hydroxycinnamosmolide was found to be less effective in inhibiting the NAT activity than the partially purified extract, suggesting either a synergistic effect with the other minor products of the extract or that there is another compound that is more effective. Previous studies have found drimane sesquiterpenoids to exhibit a range of biological activities[13], leading us to consider them as potential antifungal agents[14].

1.4 Synthesis of (-)-Drimenol and analogues

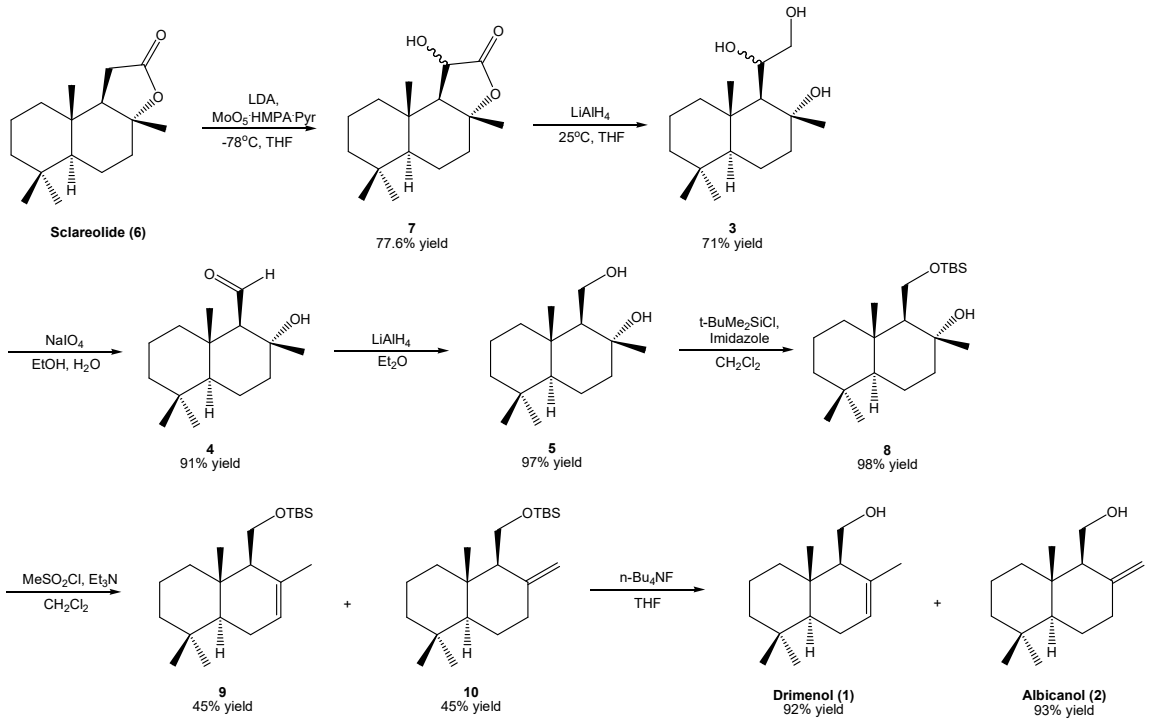

Scheme 1. Synthetic route for (-)-drimenol and analogues

The drimane sesquiterpenoids were synthesized from the commercially available 3a*R*-(+)-sclareolide (**6**) following a previously reported method published from the Hua laboratory[15]. Compound **6** was hydroxylated using lithium diisopropylamide (LDA) in tetrahydrofuran (THF) at -78°C treated with MoO_5●pyridine●HMPA (MoOPH) complex to afford a mixture of α- and β- isomers of hydroxylactone **7**. The molybdenum peroxide reagent, MoOPH, was previously reported to facilitate the direct hydroxylation of α-methylenes[16] and was used here for the production of the hydroxylactones. The two stereoisomeric products were separatable by silica gel column chromatography, but it is not necessary because the stereogenic center at C1 is destroyed after the reduction with lithium aluminum hydride (LAH) in THF at room temperature to afford triol **3**. Compound **3** was then treated with sodium periodate in ethanol and water at room temperature to perform an oxidative cleavage of the vicinal diol to produce the β-hydroxy aldehyde **4**. Compound **4** was then reduced with LAH in diethyl ether at 0°C to afford drimane-8a,11-diol **5**. The primary alcohol on **5** was then protected with *tert*-butyldimethylsilyl chloride and imidazole in dichloromethane (DCM), and elimination of the tertiary alcohol was performed using methanesulfonyl chloride and triethylamine in DCM. The tri- and di-substituted bicyclic alkene precursors **9** and **10** (**Scheme 2**) are produced because of the thermodynamically and kinetically favorable reactions, respectively. The more thermodynamically favored product **9** is a result of the deprotonation of the methyl group, where the kinetic type **10** is formed from the deprotonation of the β-methylene group. Interestingly, a 1:1 ratio of the two was obtained. The two alkenes were then separated by column chromatography and desilylation of each was performed using tetra-*n*-butylammonium fluoride (TBAF) to afford (-)-drimenol (**1**) and (+)-albicanol (**2**).

1.5 Results

Compounds **1** - **5** were screened for their ability to inhibit the growth of *C. albicans* strain SC5314 in our collaborator, Dr. Govindsamy Vediyappan's laboratory, Division of Biology, Kansas State University. (-)-Drimenol (**1**), (+)-albicanol (**2**), and the β-hydroxyaldehyde **4** were found to be effective with **1** being the most potent agent. Drimenol's ability to inhibit C. *auris* growth was tested against Fluconazole (FLU), a commonly used antifungal agent, over a course of 20 hours at 37ºC. The test was performed using growing *C. auris* cells in 200 µL of RPMI medium distributed among honeycomb microtiter wells, each measured at 0.07 OD_{600} using a Bioscreen-C growth monitor. Drimenol was found to be more effective at completely inhibiting fungal growth at a concentration of 60 µg/ml than FLU using that same concentration, as seen in **Figure 1** below. Absorbance of the *C. auris* control group increased with time because as the cells grow and propagate, the solution becomes cloudier and reduces transmittance. Drimenol was found to inhibit and kill *C. albicans* cells at concentrations ranging from 8 – 64 µg/ml and to be effective against *Aspergillus*, *Cryptococcus* and other FLU resistant strains such as *C. glabrata* and *C. krusei*.

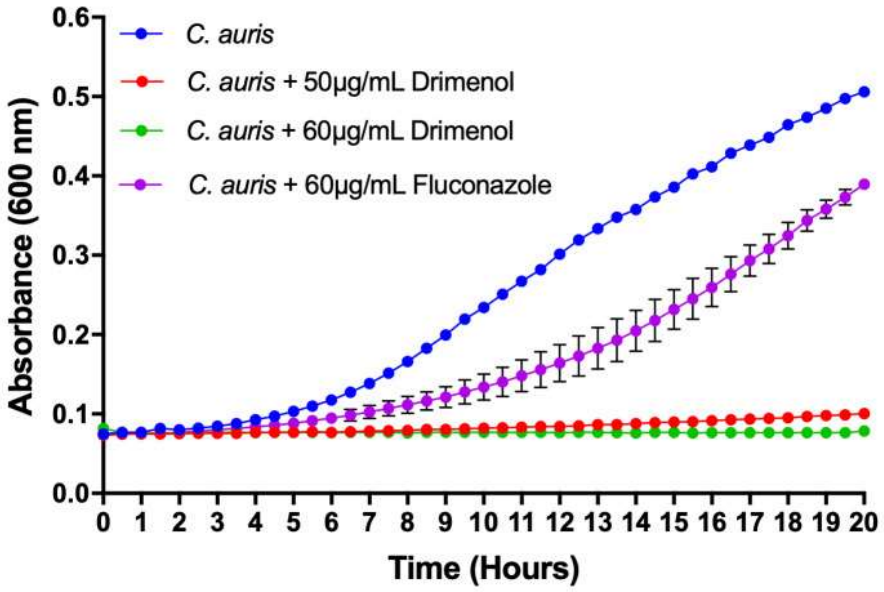

Figure 1. Effect of drimenol and fluconazole on *C. auris* growth.

Tolerance was then tested at various concentrations against *Caenorhabditis elegans* (roundworms) that were cultured with *C. albicans*. The worms were protected from fungal-mediated death and tolerated the presence of drimenol up to a concentration of 100 µg/ml with a 94% survival rate. **Figure 2** shows results of incubating the worms with 50 mg/ml of drimenol at 30°C for 2 - 3 days. The worms cultured in the wells that contained drimenol were found to be alive, judging by their movement under a microscope. The worms cultured without drimenol were immobile and most likely dead. Using a *S. albicans* mutant spot assay, the mechanism of action was determined to involve targeting protein trafficking between Golgi to ER (*RET 2*), protein secretion (Sec system) and cell signaling (*orf19.759)*, and possibly through cell division related kinase 1, Crk1.

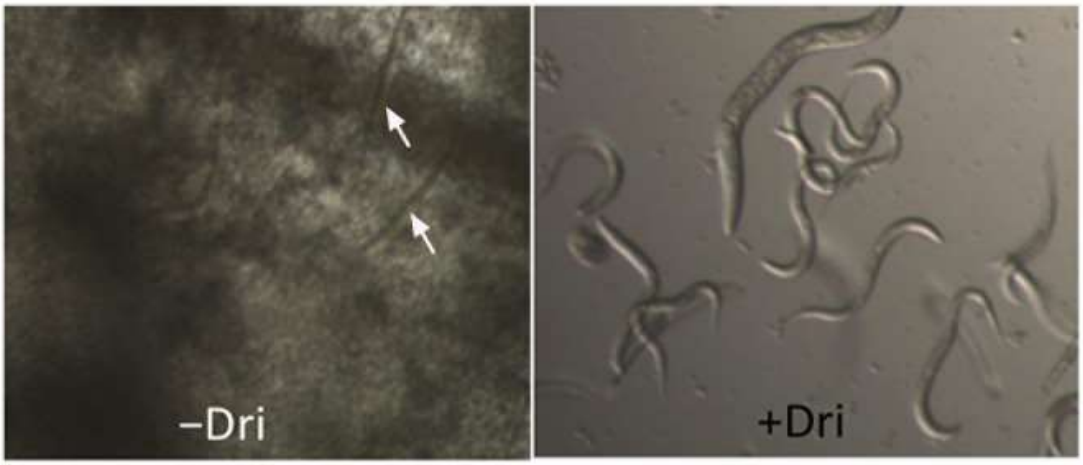

Figure 2. Drimenol tolerance test with *Caenorhabditis elegans*.

C. albicans fed larvae incubated in RPMI medium with 50 µg/ml of drimenol on the right panel and without drimenol on the left.

1.6 Experimental Procedure

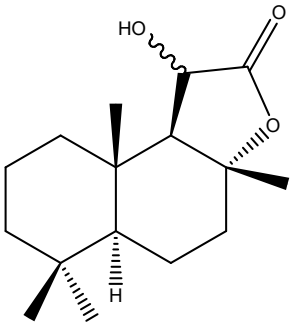

(1S,3aR,5aS,9aS,9bR)-1-Hydroxy-dodecahydro-3a,6,6,9a-tetramethylnaphtho-[2,1-b]furan-2-one and (1R,3aR, 5aS,9aS,9bR)-1-Hydroxy-dodecahydro-3a,6,6,9a-tetramethylnaphtho[2,1-b]furan-2-one **(7).** To a cold (−78 °C) solution of 1.02 mL (7.79 mmol) of diisopropylamine in 40 mL of THF under argon was added 6.36 mL (7.19 mmol) of *n*-BuLi (1.6 M in hexane). The solution was stirred at −78 °C for 1 h, and a solution of 1.50 g (5.99 mmol) of (+)-sclareolide (**6**) in 20 mL of THF was added via cannula dropwise. The solution was stirred at −78 °C for 1 h,

added to 5.10 g (0.012 mol) of MoO_5·pyridine·HMPA, and stirred for 30 min. The mixture was diluted with saturated aqueous Na_2SO_3 and extracted three times with ethyl acetate, and the organic layer was washed with water and brine, dried (Na_2SO_4), concentrated, and column chromatographed on silica gel using a mixture of hexane/ether (9:1) as an eluent to give 1.05 g (65.6% yield) of the **α-isomer** and 0.20 g (12% yield) of the **β-isomer** along with 0.296 g (20% recovery) of **6**. Spectral data is in agreement with that reported **[15]**.

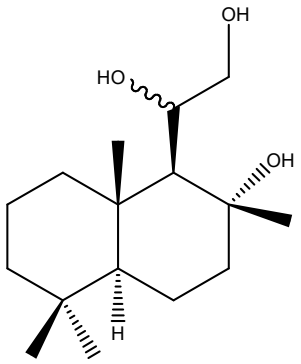

1-[(1ʻS) and (1ʻR)-1,2-Dihydroxyethyl)]-(1R,2R,4aS, 8aS)-decahydro-2,5,5,8a-tetramethyl-naphthalen-2-ol **(3).** To a solution of 0.90 g (3.4 mmol) of **7** in 20 mL of THF under argon was added 0.66 g (17.3 mmol) of $LiAlH_4$, and the mixture was stirred for 4 h at 25 °C. To it, 60 mL of water and 16 mL of 1 N HCl were added, and the solution was extracted with diethyl ether three times (50 mL each). The combined ether extracts were washed with brine, dried ($MgSO_4$), concentrated, and column chromatographed on silica gel using a gradient mixture of hexane and ethyl acetate as an eluent to give 0.65 g (71% yield) of triol **3** and 0.27 g (30% yield) of lactol byproduct. Spectral data is in agreement with that reported **[15]**.

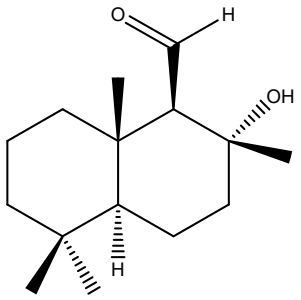

(1R,2R,4aS,8aS)-2-Hydroxy-2,5,5,8a-tetramethyl-decahydro-naphthalene-1-carbaldehyde (4).

A 0.19 g (0.81 mmol) potassium periodate were added to a solution of 0.20 g (0.74 mmol) triol **3** [15] in 10 ml THF and 2.5 ml water. The resulting mixture was stirred at 25°C for 4 hours, diluted with water (50 ml) and extracted three times with ethyl acetate (50 ml each). The combined extracts were washed with water and brine, dried (anhydrous Na_2SO_4), concentrated, and column chromatographed on silica gel using a mixture of hexane and ethyl acetate (20:1) as an eluent, yielding 0.16 g (91% yield) compound **4**, whose spectral data is in agreement with that reported **[15]**.

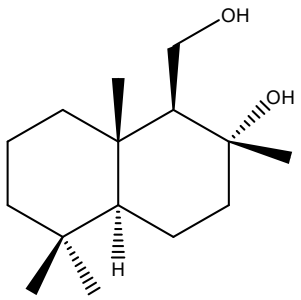

(1S,2R,4aS,8aS)-1-(Hydroxymethyl)-2,5,5,8a-tetramethyl-deca-hydronaphthalen-2-ol (5)

To a cold (0°C) solution of 1.0 g (4.2 mmol) aldehyde **4** in 80 ml of diethyl ether under argon, 80 mg (2.1 mmol) lithium aluminum hydride were added in portions. The resulting solution was stirred at 0°C for 30 minutes, diluted with aqueous NH_4Cl, and extracted with diethyl ether three times (50 ml each). The combined extracts were washed with water and brine, dried ($MgSO_4$),

and concentrated, yielding 0.98 g (97% yield) diol **5**, whose spectral data are in agreement with that reported **[15]**.

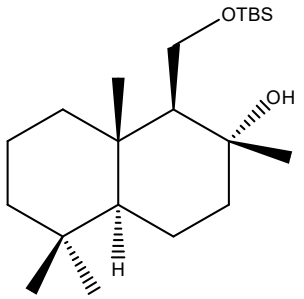

[(1S,2R,4aS,8aS)-1-(tert-Butyldimethylsilyloxymethyl)-decahydro-2,5,5,8a-tetramethylnaphthalen-2-ol] (8). To a cold (0 °C) solution of 0.90 g (3.8 mmol) of diol **5** and 1.0 g (15 mmol) of imidazole in 5.0 mL of DMF under argon was added a solution of 0.62 g (4.1 mmol) of *tert*-butyldimethylsilyl chloride in 6 mL of DMF. After stirring at 25 °C for 2 h, the reaction mixture was diluted with water and extracted three times with ethyl acetate. The combined ethyl acetate layer was washed with brine, dried (Na_2SO_4), concentrated, and column chromatographed on silica gel using a mixture of hexane/ethyl acetate (10:1) as an eluent to give 1.3 g (98% yield) of **8**: Spectral data is in agreement with that reported **[15]**.

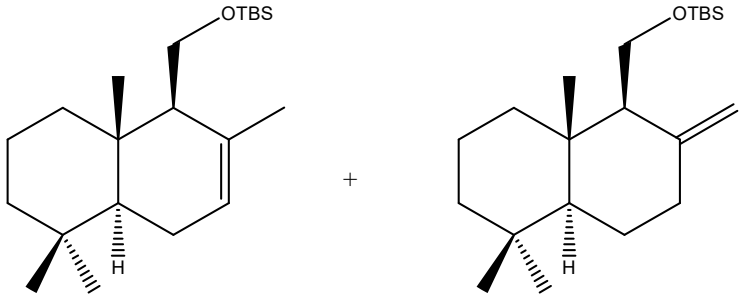

[(1S,4aS,8aS)-1-(tert-Butyldimethylsilyloxymethyl)-1,4,4a,5,6,7,8,8a-octahydro-2,5,5,8a-tetramethylnaphthalene] (9) and [(1S,4aS,8aS)-1-(tert-Butyldimethylsilyloxymethyl)-3H-1,4,4a,5,6,7,8,8a-octahydro-2-methylene-5,5,8a-trimethylnaphthalene] (10). To a cold (0 °C)

solution of 1.0 g (2.8 mmol) of **8** in 5 mL of THF under argon were added 1.4 g (14 mmol) of triethylamine and 0.48 g (4.2 mmol) of methanesulfonyl chloride. After stirring at 25 °C for 4 h, the reaction mixture was diluted with cold water and extracted three times with ethyl acetate. The combined extract was washed with water and brine, dried (Na_2SO_4), concentrated, and column chromatographed on silica gel using hexane as an eluent to give 0.42 g (45% yield) of **9** and 0.42 g (45% yield) of **10**. Spectral data is in agreement with that reported **[15].**

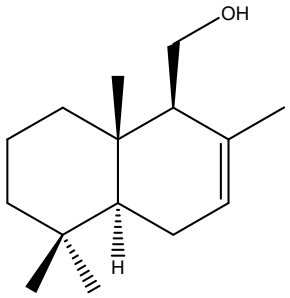

(−)-*Drimenol (1)*. A solution of 0.50 g (1.5 mmol) of **9** and 2.0 mL (2 mmol) of *n*-Bu_4NF (1.0 M in THF) was stirred under argon at 25 °C for 36 h, diluted with aqueous NH_4Cl, and extracted with ethyl acetate twice. The combined extract was washed with water and brine, dried (Na_2SO_4), concentrated, and column chromatographed on silica gel using a mixture of hexane/ethyl acetate (5:1) as an eluent to give 0.304 g (92% yield) of **1**: ^1H and ^{13}C NMR spectral data is in agreement with that reported **[15].**

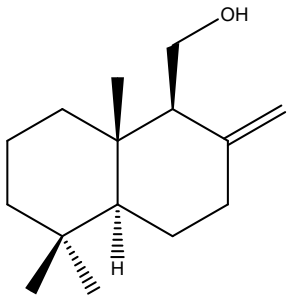

***(1S,4aS,8aS)-3H-2-Methylene-1,4,4a,5,6,7,8,8a-octahydro-5,5,8a-trimethylnaphthalene-1-methanol (2) [(+)-Albicanol]*.** A similar reaction procedure as that described above (**1**) was followed, and a 93% yield of **2** was obtained. Spectral data is in agreement with that reported **[15]**.

Chapter 2 - Synthesis and Characterization of Chiral Substituted Polyvinylpyrrolidones

2.1 Introduction

Catalytic oxidation reactions are commonly used in a wide range of industrial reactions and processes. The North American Catalysis Society estimated that 35% of the global gross domestic product (GDP) depends on catalysis and the market is increasing 5% per year[17]. Selective oxidations aid in the functionalization of compounds for drug development and total oxidations are useful in speeding up the degradation of pollutants[18]. For example, the catalytic oxidation of toxic volatile organic compounds (VOCs) produced as a byproduct of chemical industries, food processing plants, and petrochemical processing facilities have been found to be an ecofriendly and feasible way to eliminate them[19]. Catalytic approaches towards chemical reactions have many advantages such as the use of less toxic or corrosive chemicals, shorter reaction times, minimization of undesirable byproducts, and the use of less chemicals causing less hazardous waste and pollution[20–22].

2.2 Effects of Bimetallic Nanoclusters

Previous studies found that the size of the catalyst plays a major role in selectivity and reactivity because decreasing the size of the catalysts increases surface area allowing for more reaction sites[23]. Efficiency can further be increased by the addition of another metal to produce bimetallic nanoparticles that may exhibit catalytic properties that are not achievable by their monometallic

counterparts[24]. For example, the direct synthesis of hydrogen peroxide H_2O_2 from H_2 and O_2 with palladium based catalysts was found to show a higher selectivity for the formation of H_2O and degradation of H_2O_2[25]. The incorporation of gold into the nanoclusters increased selectivity of H_2O_2 formation from 34% using 5.0 wt% Pd to 80% using 2.5 wt% Pd and 2.5 wt% Au/C catalyst. Due to gold having a higher reduction potential than palladium, 1.69 V in aqueous solutions versus 0.92 V for Pd, electron density is pulled towards Au particles making the exposed Pd atoms more electrophilic.

2.3 Poly(*N*-vinyl-2-pyrrolidone) Supported Nanoclusters

Ligands and polymers are often used as stabilizers for metallic nanoparticles. They are capable of both controlling the reduction rate of the metals and preventing the aggregation of the metal atoms in solution[24]. Tsukuda et al reported that PVP stabilized Au clusters (<1.5 nm) exhibited higher catalytic activity than their larger counterparts and poly(allylamine) (PAA) supported nanoclusters for the aerobic oxidation of alcohols[26]. Their studies found that PVP not only acts as a stabilizer but also regulates the electronic structure of the Au particles by donating electron density. They proposed that the Au particles would donate electrons into the low unoccupied molecular orbitals (LUMO) of O_2 to generate the superoxo- or peroxo- species that will play a key role in the oxidation process as seen in **Figure 3**. Although the catalytic activity of polymer supported nanoclusters is well understood, there is still a gap in knowledge on enantioselective oxidations.

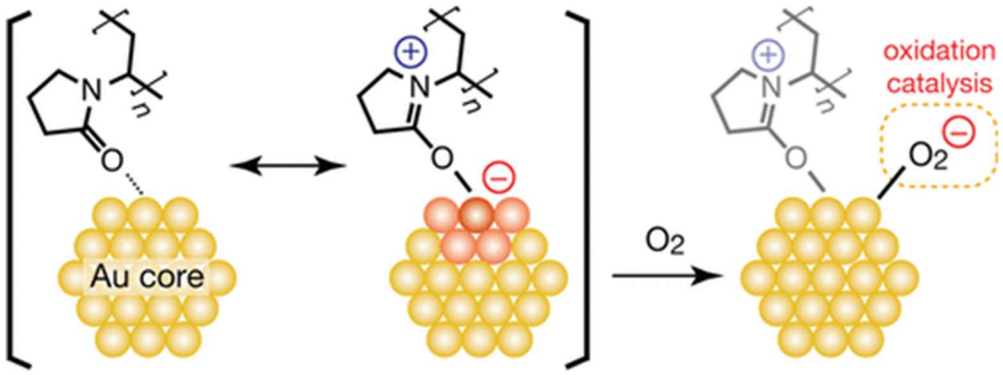

Figure 3. Proposed mechanism for the activation of molecular oxygen by Au:PVP.

Reprinted with permission from {*J. Am. Chem. Soc.* 2009, 131, 20, 7086–7093}.
Copyright © 2009, American Chemical Society

In 2016, the Hua group developed a new class of chiral C5-substituted poly-*N*-vinylpyrrolidinones (CSPVP) from L-amino acids as a stabilizer for Pd/Au and Cu/Au nanoclusters[27]. The CSPVP supported nanoclusters were then used to perform asymmetric oxidations on 1,3- and 1,2-cycloalkane diols, dihydroxylations on alkenes, and C-H oxidations on cycloalkanes (**Figure 4**). They reported excellent yields and enantioselectivities when compared to the achiral PVP counterpart. Using Pd/Au-CSPVP, they oxidized *trans* and meso-*cis* diols under atmospheric oxygen to selectively give (*S*)-hydroxy ketones. Both *trans*- and *cis*-alkenes were oxidized under 30 psi oxygen to give syn diols as the major product and Cu/Au-CSPVP was used to oxidize cycloalkanes to chiral cycloalkanones.

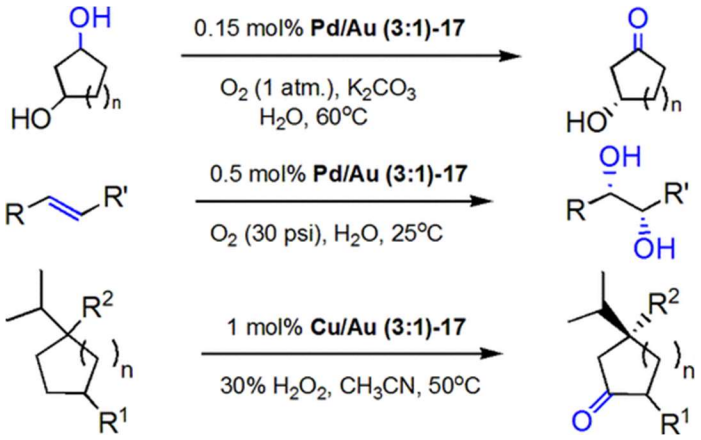

Figure 4. Representative asymmetric oxidations previously reported by Hua et al., 2016.

Reprinted with permission from {*J. Am. Chem. Soc. 2016, 138, 51, 16839–16848*}.
Copyright © 2016, American Chemical Society

2.4 Discussion

Synthesis of C3-Substituted Poly-*N*-vinylpyrrolidinone

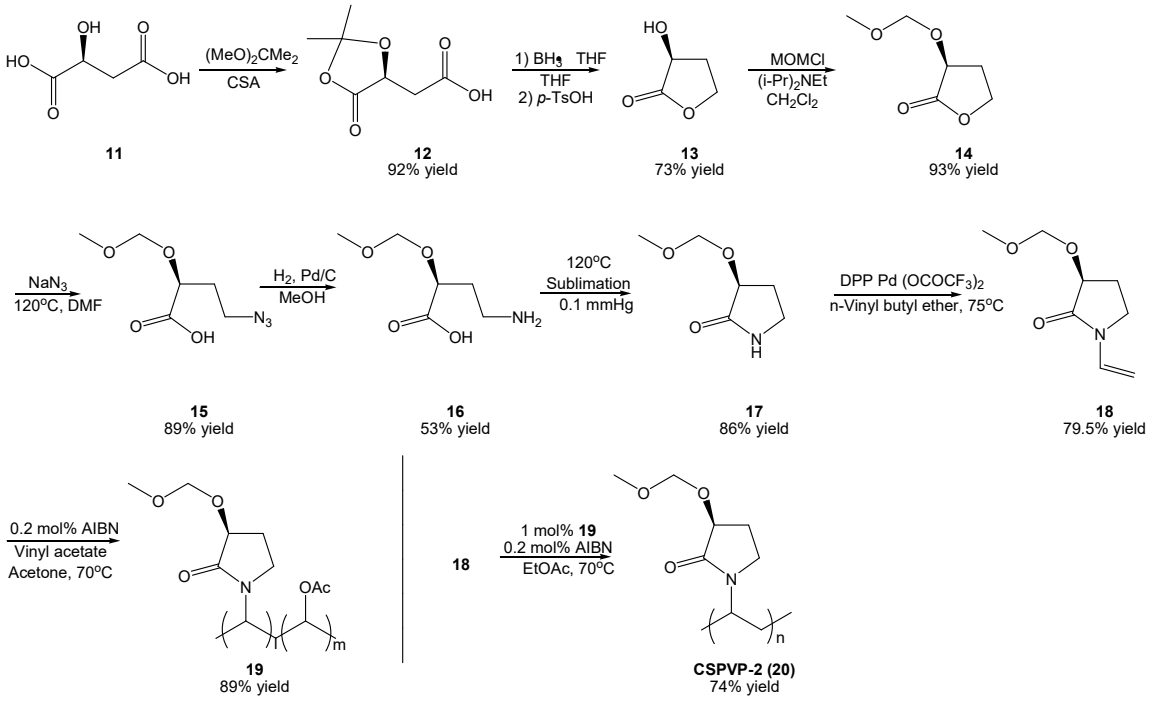

Scheme 2. Synthetic pathway for CSPVP-2 (**20**)

To further investigate the effect of CSPVP supported nanoclusters on asymmetric oxidations, a C3 substituted polymer was synthesized from L-(*S*)-malic acid. The dicarboxylic acid **11** was treated with a catalytic amount of D-10-camphorsulfonic acid (CSA) in 2,2-dimethoxypropane to give the acetonide acid **12**. The carboxylic acid group on compound **12** was reduced using borane THF complex (BH_3•THF) then upon acidification with catalytic *p*-toluenesulfonic acid (*p*-TsOH), the molecule cyclized to furnish α-hydroxylactone **13**. The cyclization occurs because the carbonyl oxygen gets protonated, causing the carbonyl carbon to become more electrophilic. The primary hydroxyl group would perform an intramolecular nucleophilic attack on that carbon to break the bond between it and the adjacent oxygen and release the acetonide protecting group into solution as acetone. The cyclization could also be performed using CSA as the proton source instead of *p*-TsOH but it must then be quenched with sodium acetate upon work-up. The hydroxyl group on **13** was then alkylized using chloromethyl methyl ether (MOMCl) and diisopropylethylamine (DIPEA) at 0°C to produce (*S*)-2-(methoxymethoxy)butanolide **14**. The order of addition here is important because when the DIPEA was added before the MOMCl, the yield was 61% but when the order is reversed the yield increased to 93%. Compound **14** was treated with sodium azide in DMF to produce the azido-acid **15**, then hydrogenated under 30 psi hydrogen with 5% Pd/C in methanol to produce the amino acid **16** with some recovered **14**. The yield for this step was moderate either because compound **15** contained some starting material or the amine could have also been hydrogenated. If this was the case, the hydroxy group on the carboxylic end would attack the methylene adjacent to the nitrogen and kick out the amine group as ammonia to generate lactone **14**. Upon sublimation of **16** under reduced pressure at 120°C, compound **16** cyclizes to produce the MOM-substituted lactam **17**. Lactam **17** was then vinylized in n-butyl vinyl ether with catalytic 4,7-diphenyl-1,10-phenanthroline palladium

bis(trifluoroacetate) [(DPP)Pd($OCOCF_3$)$_2$] to produce the vinyl lactam monomer **18**. Vinyl lactam **18** was copolymerized in acetone with vinyl acetate and catalytic azobisisobutyronitrile (AIBN) in a sealed tube under nitrogen atmosphere. The copolymer **19** was then used to polymerize vinyl lactam **18** with the aid of AIBN as the radical initiator to give the C3 substituted polymer **20**. A direct correlation between the polymer length and the mole percent of AIBN used was observed whereas the amount of AIBN used increases, the general length of the polymer obtained decreased. Using 0.2 mol% of AIBN, the polymer weight was approximately 80,000 amu but when 0.4 mol% was used the weight was roughly halved. Polymer length was determined using high resolution mass spectroscopy to obtain the exact molecular weight which could then be used to calculate length.

2.5 Conclusion

The C3-Substituted poly-*N*-vinylpyrrolidinone was synthesized and used as a polymer for Pd/Au and Cu/Au nanoclusters for oxidation. Upon verification of the enantioselective properties of the polymer, further studies can be done to increase its synthetic usefulness. Further modification of the C3 substituent such as the addition of a phenyl, isobutyl, or cyclopentyl group could potentially increase enantioselectivity of the catalysts. Our work was recently published in The Journal of Organic Chemistry (https://doi.org/10.1021/acs.joc.2c00449).[28]

2.6 Experimental Procedure

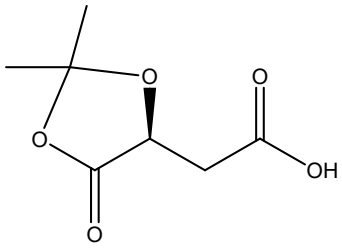

(S)-2-(2,2-Dimethyl-5-oxo-1,3-dioxolan-4-yl) acetic acid (12) (from EE-3-58)

To a solution of 300 mL 2,2-dimethoxypropane, 15.0 g (112 mmol) L-(S)-malic acid (**11**) and 0.5 g (2.15 mmol) *D*-10-camphorsulfonic acid, as a catalyst, were added. The solution was stirred for 12 h at 25 ºC with color changed to light yellow. After 0.2 g (2.378 mmol) of sodium acetate was added and stirred for 1 h, the reaction solution changed to colorless again. After the reaction mixture was filtered, the filtrate was concentrated to dryness with a rotary evaporator. The resulting residue was crystallized from a mixture of chloroform and hexane (50 mL: 100 mL) to give 17.89 g (92% yield) desired product (**12**) as a white solid. **^{1}H NMR** (400 MHz, $CDCl_3$): δ 11.2 - 10.7 (bs, 1 H, OH), 4.72 (dd, *J* = 6.8, 4.0 Hz, 1 H), 3.00 (dd, *J* = 17.2, 4 Hz, 1 H), 2.86 (dd, *J* = 17.2, 6.8 Hz, 1 H), 1.62 (s, 3 H), 1.57 (s, 3 H); **^{13}C NMR** (100 MHz, $CDCl_3$): δ 174.8, 171.9, 111.4, 70.4, 36.0, 26.8, 25.8. HRMS-ESI (positive mode): m/z $[M + H]^+$ calcd for $C_7H_{10}O_5^+$: 175.0606, found: 175.0615.

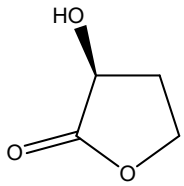

(S)-3-Hydroxy-dihydrofuran-2(3H)-one (13) (from EE-3-51)

To a flame-dried round bottom flask over an ice bath, a solution of 17.5 g (0.101 mol) (S)-2-(2,2-dimethyl-5-oxo-1,3-dioxolan-4-yl) acetic acid (**12**) dissolved in 130 mL distilled THF was added

under argon. Then, 130 mL (130 mmol) BH_3•THF (1 M solution in THF) complex was added to the solution slowly with a dropping funnel over 30 min and stirred for 12 h at 25 °C. The uncompleted reaction was detected by NMR followed by another portion of 44 mL BH_3•THF (1 M solution in THF) according to the previous method and stirred for another 8 h at 25 °C. Then, the reaction was diluted with 240 mL methanol, evaporated to dryness. After another portion of 30 mL methanol was added, the mixture was evaporated again to remove trimethyl borate. This procedure was repeated until the weight of the dryness was consistent (16.67 g). The crude was then diluted with 200 mL chloroform, added with 0.8 g (3.45 mmol) *para*-toluenesulfonic acid as a catalyst for cyclization. After the solution was stirred at 25 °C for 12 h, 0.29 g (3.45 mmol) sodium bicarbonate was added to neutralize the acid. The solution was then concentrated to dryness with a rotary evaporator, loaded to a silica gel column, eluted with a gradient solution of hexane and ethyl acetate to yield 7.54 g (73% yield) desired product (**13**) as an oil. **^{1}H NMR** (400 MHz, $CDCl_3$): δ 4.53 (dd, J = 10, 8.4 Hz, 1H), 4.44 (dt, J = 10, 7 Hz, 1H), 4.25 (ddd, J = 8.4, 6.8, 1.6 Hz, 1H), 3.8 – 3.6 (bs, 1H, OH), 2.62 (dddd, J = 10, 8, 6, 2 Hz, 1H), 2.30 (dddd, J = 10, 8.8, 8.4, 4 Hz, 1H); **^{13}C NMR** (100 MHz, $CDCl_3$): δ 178.2, 67.4, 65.3, 30.9. MS (ESI, MeOH): m/z = 103.112 ($[M + H]^+$).

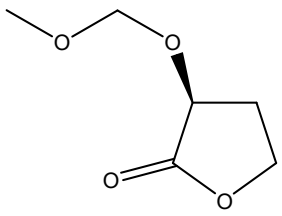

(-)-(S)-3-(Methoxymethoxy)-dihydrofuran-2(3H)-one (14) (from EE-3-110)

To a flame-dried round bottom flask over an ice bath, 2.8 g (27.5 mmol) (*S*)-3-hydroxy-dihydrofuran-2(3*H*)-one (**13**) in 20 mL dichloromethane, and 11 mL (68.8 mmol) methoxymethyl chloride (prepared by mixing dimethoxymethane and acetyl chloride with the

ratio of 1:1) was injected into the flask sequentially under argon. The solution was added with 7.2 mL (41.3 mmol) of diisopropylethylamine dropwise over 5 min with a dropping funnel, stirred at 25 ºC for 18 h. Then, the reaction mixture was quenched with 20 mL aqueous ammonium chloride solution, extracted with 20 mL dichloromethane for three times. The combined organic layer was then washed with aqueous sodium bicarbonate solution and brine, dried with sodium sulfate, concentrated with a rotary evaporator to yield 3.73 g (93% yield) desired product (**14**). Compound **14**: **^{1}H NMR** (400 MHz, $CDCl_3$): δ 4.96 (d, *J* = 6.8 Hz, 1 H), 4.73 (d, *J* = 6.8 Hz, 1 H), 4.45 (dt, *J* = 8.4, 4 Hz, 1 H), 4.41 (d, *J* = 9 Hz, 1 H), 4.24 (td, *J* = 9, 6.4 Hz, 1 H), 3.43 (s, 3 H), 2.59 (dddd, *J* = 12.8, 8.8, 6.8, 3.2 Hz, 1 H), 2.29 (dq, *J* = 12.8, 8.8 Hz, 1 H); **^{13}C NMR** (100 MHz, $CDCl_3$): δ 174.9, 95.9, 70.3, 65.2, 56.0, 29.9. MS (ESI, MeOH): m/z = 168.91 $(M+Na)^+$, 146.90 $([M + H]^+)$.

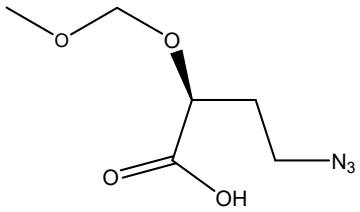

(S)-4-Azido-2-(methoxymethoxy)butanoic acid (15) (from EE-2-88)

To a dried two-neck round bottom flask equipped with a condenser, 0.98 g (15 mmol) sodium azide was added and purged with argon. Then, 1.0 g (6.85 mmol) lactone (**14**) in 5 mL dried DMF solution was added under argon. The reaction mixture was heated to 120 ºC and stirred for 24 h. After the reaction mixture was cooled to 25 ºC, 60 mL water was added to dilute the reaction mixture. The reaction mixture was then extracted with diethyl ether for three times. The combined organic layer was dried with sodium sulfate, concentrated with a rotary evaporator to give 80 mg (8% recovery) starting material. In terms of the aqueous layer, 1 N HCl was utilized to acidify the aqueous solution to pH~2. Then, the acidic aqueous layer was extracted with 40

mL dichloromethane for three times. The combined organic layer from the acidified aqueous layer was dried with sodium sulfate, concentrated with a rotary evaporator to yield 1.165 g (89% yield) desired product (**15**) as an oil, which was used for further synthesis without purification. **^{1}H NMR** (400 MHz, $CDCl_3$): δ 4.78 (d, *J* = 6.8 Hz, 1H), 4.71 (d, *J* = 6.8 Hz, 1H), 4.30 (dd, *J* = 8, 4.4 Hz, 1H), 3.53 – 3.47 (m, 2H), 3.42 (s, 3H), 2.12 – 2.05 (m, 2H); **^{13}C NMR** (100 MHz, $CDCl_3$): δ 176.3 (C=O), 96.5 (OCO), 72.5 (CHO), 56.3 (OMe), 47.3 (CH_2N), 32.0 (CH_2). MS (ESI, MeOH; negative mode): m/z = 187.982 ($[M - H]^-$). HRMS-ESI (negative mode): m/z $[M - H]^-$ calcd for $C_6H_{10}N_3O_4^-$: 188.0677, found: 188.0663.

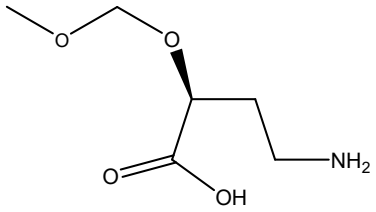

(S)-4-Amino-2-(methoxymethoxy)butanoic acid (16) (from EE-2-89)

To a hydrogenation bottle, 1.56 g (8.25 mmol) (*S*)-4-azido-2-(methoxymethoxy)butanoic acid (**15**), 0.18 g (0.0825 mmol) 5% Pd/C were mixed in 30 mL methanol. Then, the hydrogenation system was purged with hydrogen, and the reaction mixture was shaken at 25 ºC for 16 h with the hydrogen pressure of 30 psi. Then, the reaction mixture was filtered through Celite, washed with methanol. The filtration was concentrated to dryness. The dry crude produced was then washed with ether to remove impurities, and the residue was dried under vacuum with an oil pump to yield 0.798 g (53 % yield) amino acid **16**, which was used for sublimation directly without purification. **^{1}H NMR** (400 MHz, D_2O): δ 4.62 (d, *J* = 7.0 Hz, 1 H, OCH_2O), 4.56 (d, *J* = 7.0 Hz, 1 H, OCH_2O), 4.01 (dd, *J* = 6.8, 4.4 Hz, 1 H, CHO), 3.30 (s, 3 H, OMe), 3.02 (t, *J* = 7.4 Hz, 2 H, CH_2N), 2.12 – 1.80 (m, 2 H, CH_2); **^{13}C NMR** (100 MHz, D_2O): δ 178.4, 95.5, 75.9,

55.6, 36.7, 30.0; HRMS-ESI (negative mode): m/z [M - H]$^-$ calcd for $C_6H_{12}N_3O_4^-$: 162.0766, found: 162.0790.

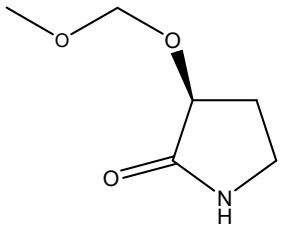

(S)-3-(Methoxymethoxy)pyrrolidin-2-one (17) (from EE-2-100)

To a sublimator, 492 mg (30. mmol) amino acid **16** was transferred to the bottom of it carefully. The sublimator was then connected to a vacuum at 0.1 mmHg, and the temperature was heated to 140 to 150 ºC gradually. The completion of sublimation was checked by lowering the oil bath level to observe if there was any white solids in the chamber. After that, the apparatus was cooled to 25 ºC and detached from the oil pump. The sublimated substance was collected and loaded to a silica gel column, eluted with a gradient mixture of hexane and dichloromethane as well as methanol to give 212 mg (49 % overall yield from lactone) desired product **17** as a white solid. **^{1}H NMR** (400 MHz, $CDCl_3$): δ 6.60 - 6.40 (bs, 1 H), 4.95 (d, *J* = 6.8 Hz, 1 H), 4.75 (d, *J* = 6.8 Hz, 1 H), 4.269 (t, *J* = 8 Hz, 1 H), 3.43 (s, 3 H), 3.46 – 3.39 (m, 1 H), 3.30 – 3.25 (m, 1 H), 2.51 – 2.42 (m, 1 H), 2.15 – 2.11 (m, 1 H); **^{13}C NMR** (100 MHz, $CDCl_3$): δ 175.7 (C=O), 96.2 (OCO), 72.8 (CHO), 55.8 (OCH_3), 38.7 (CN), 29.1 (CH_2). MS (ESI, MeOH): m/z = 146.12 ([M + H]$^+$). HRMS-ESI: m/z [M + H]$^+$ calcd for $C_6H_{12}NO_3^+$: 146.0812, found: 146.0817.

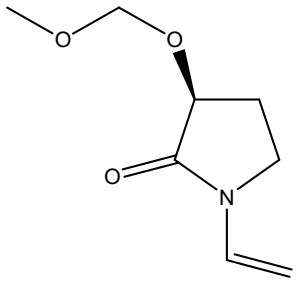

(-)-(S)-3-(Methoxymethoxy)-1-vinylpyrrolidin-2-one (18) (from EE-2-83)

To a solution of 23 mL distilled vinyl butyl ether, 199 mg (1.37 mmol) (*S*)-3-(methoxymethoxy)pyrrolidin-2-one (**17**) and 17 mg (0.027 mmol) of (DPP)Pd($OCOCF_3$)$_2$ were added. After stirred at 75 ºC for 3 hours, the reaction mixture was cooled to 25 ºC, filtered through Celite, washed with 100 mL ethyl acetate. The filtrate was then dried with sodium sulfate, concentrated to dryness, loaded to a silica gel column, flushed with a gradient mixture of hexane and ethyl acetate to yield 186 mg (79.5 % yield) of desired product **18** as a white solid. **^{1}H NMR** (400 MHz, $CDCl_3$): δ 7.09 (dd, *J* = 16, 9 Hz, 1 H), 4.98 (d, *J* = 6.8 Hz, 1 H), 4.75 (d, *J* = 6.8 Hz, 1 H), 4.51 (dd, *J* = 16, 8 Hz, 1 H), 4.39 (dd, *J* = 9, 8 Hz, 1 H), 3.60 (td, *J* = 10, 3.2 Hz, 1 H), 3.43 (s, 3 H), 3.36 (dt, *J* = 10, 7.6 Hz, 1 H), 2.51 (dtd, *J* = 11, 8, 2.8 Hz, 1 H), 2.08 (tt, *J* = 11, 8 Hz, 1 H); **^{13}C NMR** (100 MHz, $CDCl_3$): δ 170.6, 129.2 (HC=), 96.2 (OCO), 95.5 (=CH_2), 73.8 (HCO), 55.8 (OMe), 41.2 (CH_2N), 26.3 (CH_2). MS (ESI, MeOH): m/z = 172.13 ($[M + H]^+$). HRMS-ESI: m/z $[M + H]^+$ calcd for $C_6H_{12}NO_3^+$: 172.0974, found: 172.0988.

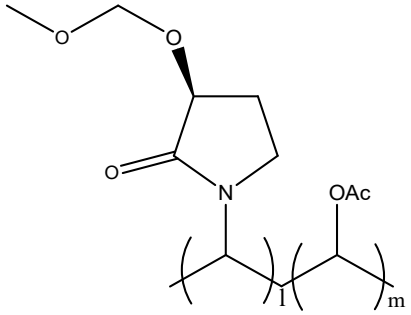

Poly((S)-3-(methoxymethoxy)-1-vinylpyrrolidin-2-one-co-vinyl acetate) [P(MVP-co-VAc)] (19) (from EE-2-86)

To a screw-sealing tube, a solution of 36 mg (0.21 mmol) dried *N*-vinylpyrrolidinone **18**, 6.5 mg (0.040 mmol) dried azobisisobutyronitrile (AIBN) in acetone and 20 mL (0.16 mmol) dried and degassed vinyl acetate in 1 mL of dried and degassed acetone were prepared in a nitrogen-purged glove box. After the tube was capped with a Teflon cap and sealed tightly by pushing an O-ring, the tube was transferred to a hood and stirred at 65 ^{o}C for 48 h. The tube was then allowed to cool to 25^{o}C, dissolved with chloroform, and stirred an even solution. The prepared solution was added into a vigorously stirring solution of pentane dropwise. The white precipitate was collected by filtration, washed with pentane, and dried under vacuum to give 48 mg (89% yield) of copolymer **19** as white solids. $[\alpha]_D^{22}$ = -168.0 (c 0.5, $CHCl_3$); **^{1}H NMR** (400 MHz, $CDCl_3$): δ 5.0 – 4.75 (bm, 1 H), 4.74 – 4.60 (bs, 1 H), 4.33 – 4.20 (bs, 1 H), 3.95 – 3.0 (bm, 2 H), 3.38 (s, 3 H), 2.50 – 2.25 (bs, 1 H), 2.15 – 1.30 (bm, 4 H); **^{13}C NMR** (100 MHz, $CDCl_3$): δ 172.9, 96.4, 96.1, 95.9, 74.7, 74.1 (2 C), 55.6, 45.2, 44.1, 43.7, 39.5, 39.2, 38.6, 36.0 – 31.0 (m), 27.

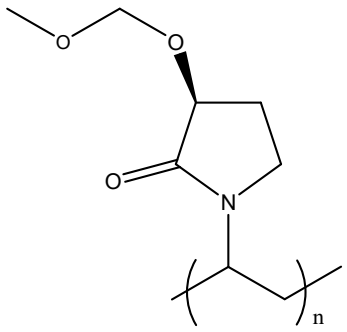

Poly[3-(methoxymethoxy)-1-vinylpyrrolidin-2-one] (20) (from EE-2-128)

To a screw-sealing tube, a solution of 171 mg (1.0 mmol) vinyl lactam **18**, 1.71 mg copolymer **19**, 0.67 mg (4.0 mmol, 0.4 mol%) AIBN in 2 mL of ethyl acetate was prepared in a glove box

purged with nitrogen. After the tube was capped with a Teflon cap and sealed tightly by pushing a Teflon O-ring, the tube was then transferred to a hood and stirred at 75 °C for 48 h. After the reaction mixture was cooled to 25 °C, the reaction mixture was dissolved with chloroform and stirred to an even solution. The solution was then added to a solution of pentane dropwise with white solid precipitated. The white solid was then collected by filtration, dried under vacuum to give 0.125 g (74% yield) of chiral polymer **20** as a white solid. $[\alpha]_D^{22}$ = -168.0 (c 0.5, $CHCl_3$); **^{1}H NMR** (400 MHz, $CDCl_3$): δ 5.0 – 4.75 (bm, 1 H), 4.74 – 4.60 (bs, 1 H), 4.33 – 4.20 (bs, 1 H), 3.95 – 3.0 (bm, 2 H), 3.38 (s, 3 H), 2.50 – 2.25 (bs, 1 H), 2.15 – 1.30 (bm, 4 H); **^{13}C NMR** (100 MHz, $CDCl_3$): δ 172.9, 96.4, 96.1, 95.9, 74.7, 74.1 (2 C), 55.6, 45.2, 44.1, 43.7, 39.5, 39.2, 38.6 (3 C), 36.0 – 31.0 (m), 27.1.

References

(1) R, T. S. World AIDS Day [2]. *SA Pharm. J.* **2010**, *77* (1), 57.

(2) White, P. L.; Dhillon, R.; Cordey, A.; Hughes, H.; Faggian, F.; Soni, S.; Pandey, M.; Whitaker, H.; May, A.; Morgan, M.; Wise, M. P.; Healy, B.; Blyth, I.; Price, J. S.; Vale, L.; Posso, R.; Kronda, J.; Blackwood, A.; Rafferty, H.; Moffitt, A.; Tsitsopoulou, A.; Gaur, S.; Holmes, T.; Backx, M. Clinical Infectious Diseases. *Clin. Infect. Dis.* ® **2021**, *73* (7), 1634–1678. https://doi.org/10.1093/cid/ciaa1298.

(3) Satoh, K.; Makimura, K.; Hasumi, Y.; Nishiyama, Y.; Uchida, K.; Yamaguchi, H. Candida Auris Sp. Nov., a Novel Ascomycetous Yeast Isolated from the External Ear Canal of an Inpatient in a Japanese Hospital. *Microbiol Immunol* **2009**, *53*, 41–44. https://doi.org/10.1111/j.1348-0421.2008.00083.x.

(4) Kim, M. N.; Shin, J. H.; Sung, H.; Lee, K.; Kim, E. C.; Ryoo, N.; Lee, J. S.; Jung, S. L.; Park, K. H.; Kee, S. J.; Kim, S. H.; Shin, M. G.; Suh, S. P.; Ryang, D. W. Candida Haemulonii and Closely Related Species at 5 University Hospitals in Korea: Identification, Antifungal Susceptibility, and Clinical Features. *Clin. Infect. Dis.* **2009**, *48* (6). https://doi.org/10.1086/597108.

(5) Khan, Z. U.; Al-Sweih, N. A.; Ahmad, S.; Al-Kazemi, N.; Khan, S.; Joseph, L.; Chandy, R. Outbreak of Fungemia among Neonates Caused by Candida Haemulonii Resistant to Amphotericin B, Itraconazole, and Fluconazole. *J. Clin. Microbiol.* **2007**, *45* (6), 2025–2027. https://doi.org/10.1128/JCM.00222-07.

(6) Lockhart, S. R.; Etienne, K. A.; Vallabhaneni, S.; Farooqi, J.; Chowdhary, A.; Govender, N. P.; Lopes Colombo, A.; Calvo, B.; Cuomo, C. A.; Desjardins, C. A.; Berkow, E. L.; Castanheira, M.; Magobo, R. E.; Jabeen, K.; Asghar, R. J.; Meis, J. F.; Jackson, B.; Chiller, T.; Litvintseva, A. P. Clinical Infectious Diseases Simultaneous Emergence of Multidrug-Resistant Candida Auris on 3 Continents Confirmed by Whole-Genome Sequencing and Epidemiological Analyses. *Clin. Infect. Dis.* ® **2017**, *64* (2), 134–174. https://doi.org/10.1093/cid/ciw691.

(7) Calvo, B.; Melo, A. S. A.; Perozo-Mena, A.; Hernandez, M.; Francisco, E. C.; Hagen, F.; Meis, J. F.; Colombo, A. L. First Report of Candida Auris in America: Clinical and Microbiological Aspects of 18 Episodes of Candidemia. *J. Infect.* **2016**, *73* (4), 369–374. https://doi.org/10.1016/j.jinf.2016.07.008.

(8) Chowdhary, A.; Kumar, V. A.; Sharma, & C.; Prakash, A.; Agarwal, K.; Babu, R.; Dinesh, K. R.; Karim, S.; Singh, S. K.; Hagen, F.; Meis, J. F. Multidrug-Resistant Endemic Clonal Strain of Candida Auris in India. *Eur J Clin Microbiol Infect Dis* **2013**, *33*, 919–926. https://doi.org/10.1007/s10096-013-2027-1.

(9) Rindidzani E. Magobo, Craig Corcoran, Sharona Seetharam, and N. P. G. Candida Auris–Associated Candidemia, South Africa. *Emerg. Infect. Dis.* **2014**, *20*, 1250–1251. https://doi.org/10.3201/eid2007.131654.

(10) Emara, M.; Ahmad, S.; Khan, Z.; Joseph, L.; Al-obaid, I.; Purohit, P. Candida Auris Candidemia in Kuwait, 2014. *Emerg. Infect. Dis.* **2015**, *21* (6), 1091–1092.

(11) Madikane, V. E.; Bhakta, S.; Russell, A. J.; Campbell, W. E.; Claridge, T. D. W.; Elisha, B. G.; Davies, S. G.; Smith, P.; Sim, E. Inhibition of Mycobacterial Arylamine N-Acetyltransferase Contributes to Anti-Mycobacterial Activity of Warburgia Salutaris. *Bioorganic Med. Chem.* **2007**, *15* (10), 3579–3586. https://doi.org/10.1016/j.bmc.2007.02.011.

(12) Evans, D. A. P., Manley, K. A. and McKuisick, V. A. Genetic Control of Isoniazid Metabolism in Man. *J. Cell Biol.* **1963**, *16* (53), 513–520. https://doi.org/10.1083/jcb.16.3.513.

(13) Jansen, B. J. M.; De Groot, A. Occurrence, Biological Activity and Synthesis of Drimane Sesquiterpenoids. https://doi.org/10.1039/b311170a.

(14) Edouarzin, E.; Horn, C.; Paudyal, A.; Zhang, C.; Lu, J.; Tong, Z.; Giaever, G.; Nislow, C.; Veerapandian, R.; Hua, D. H.; Vediyappan, G. Broad-Spectrum Antifungal Activities and Mechanism of Drimane Sesquiterpenoids. *Microb. Cell* **2020**, *7* (6). https://doi.org/10.15698/mic2020.06.719.

(15) Hua, D. H.; Huang, X.; Chen, Y.; Battina, S. K.; Tamura, M.; Noh, S. K.; Koo, S. I.; Namatame, I.; Tomoda, H.; Perchellet, E. M.; Perchellet, J. P. Total Syntheses of (+)-Chloropuupehenone and (+)-Chloropuupehenol and Their Analogues and Evaluation of Their Bioactivities. *J. Org. Chem.* **2004**, *69* (18), 6065–6078. https://doi.org/10.1021/jo0491399.

(16) Vedejs, E.; Engler, D. A.; Telschow, J. E. Transition-Metal Peroxide Reactions. Synthesis of α-Hydroxycarbonyl Compounds from Enolates. *J. Org. Chem.* **1978**, *43* (2), 188–196. https://doi.org/10.1021/jo00396a002.

(17) David J. Cole-Hamilton, R. P. T. Homogeneous Catalysis—Advantages and Problems,. In *Catalyst Separation, Recovery and Recycling*; 2006; p 1.

(18) Valange, S.; Védrine, J. C. General and Prospective Views on Oxidation Reactions in Heterogeneous Catalysis. *Catalysts* **2018**, *8* (10). https://doi.org/10.3390/catal8100483.

(19) Song, S.; Zhang, S.; Zhang, X.; Verma, P.; Wen, M. Advances in Catalytic Oxidation of Volatile Organic Compounds over Pd-Supported Catalysts: Recent Trends and Challenges. https://doi.org/10.3389/fmats.2020.595667.

(20) Kani, I.; Kurtça, M. Synthesis, Structural Characterization, and Benzyl Alcohol Oxidation Activity of Mononuclear Manganese(II) Complex with 2,2'-Bipyridine: [Mn(Bipy)2(ClO4)2]. *Turkish J. Chem.* **2012**, *36* (6), 827–840. https://doi.org/10.3906/kim-1110-4.

(21) Gallezot, P. Selective Oxidation with Air on Metal Catalysts. *Catal. Today* **1997**, *37* (4), 405–418. https://doi.org/10.1016/S0920-5861(97)00024-2.

(22) Sanjay, S.; Kumar, A. New Strategies for the Oxidation of Some Industrial Materials under Microwave Irradiation Using Ag and Cu Metal Ions and Their Nanoparticles. **2018**, *05* (07), 614–625.

(23) Hemalatha, K.; Madhumitha, G.; Kajbafvala, A.; Anupama, N.; Sompalle, R.; Mohana Roopan, S. Function of Nanocatalyst in Chemistry of Organic Compounds Revolution: An Overview. *J. Nanomater.* **2013**, *2013*. https://doi.org/10.1155/2013/341015.

(24) Toshima, N.; Yonezawa, T. Bimetallic Nanoparticles - Novel Materials for Chemical and Physical Applications. *New J. Chem.* **1998**, *22* (11), 1179–1201. https://doi.org/10.1039/a805753b.

(25) Junjie Gu, Suli Wang, Zhiyuan He, You Han, J. Z. Direct Synthesis of Hydrogen Peroxide from Hydrogen and Oxygen over Activated-Carbon-Supported Pd-Ag Alloy Catalysts. *Catal. Sci. Technol.* **1983**, *6* (3), 385. https://doi.org/10.1016/0166-9834(83)80125-0.

(26) Tsunoyama, H.; Ichikuni, N.; Sakurai, H.; Tsukuda, T. Effect of Electronic Structures of Au Clusters Stabilized by Poly (N -Vinyl-2-Pyrrolidone) on Aerobic Oxidation Catalysis. *J. Am. Chem. Soc.* **2009**, *131* (20), 7086–7093.

(27) Hao, B.; Gunaratna, M. J.; Zhang, M.; Weerasekara, S.; Seiwald, S. N.; Nguyen, V. T.; Meier, A.; Hua, D. H. Chiral-Substituted Poly-N-Vinylpyrrolidinones and Bimetallic Nanoclusters in Catalytic Asymmetric Oxidation Reactions. *J. Am. Chem. Soc.* **2016**, *138* (51), 16839–16848. https://doi.org/10.1021/jacs.6b12113.

(28) Fan, H.; Tong, Z.; Ren, Z.; Mishra, K.; Morita, S.; Edouarzin, E.; Gorla, L.; Averkiev, B.; Day, V. W.; Hua, D. H. Synthesis and Characterization of Bimetallic Nanoclusters Stabilized by Chiral and Achiral Polyvinylpyrrolidinones. Catalytic C(sp^3)-H Oxidation. *J. Org. Chem*. **2022**, online: https://doi.org/10.1021/acs.joc.2c00449.

Appendix A -

1H and 13C NMR spectra of synthesized molecules

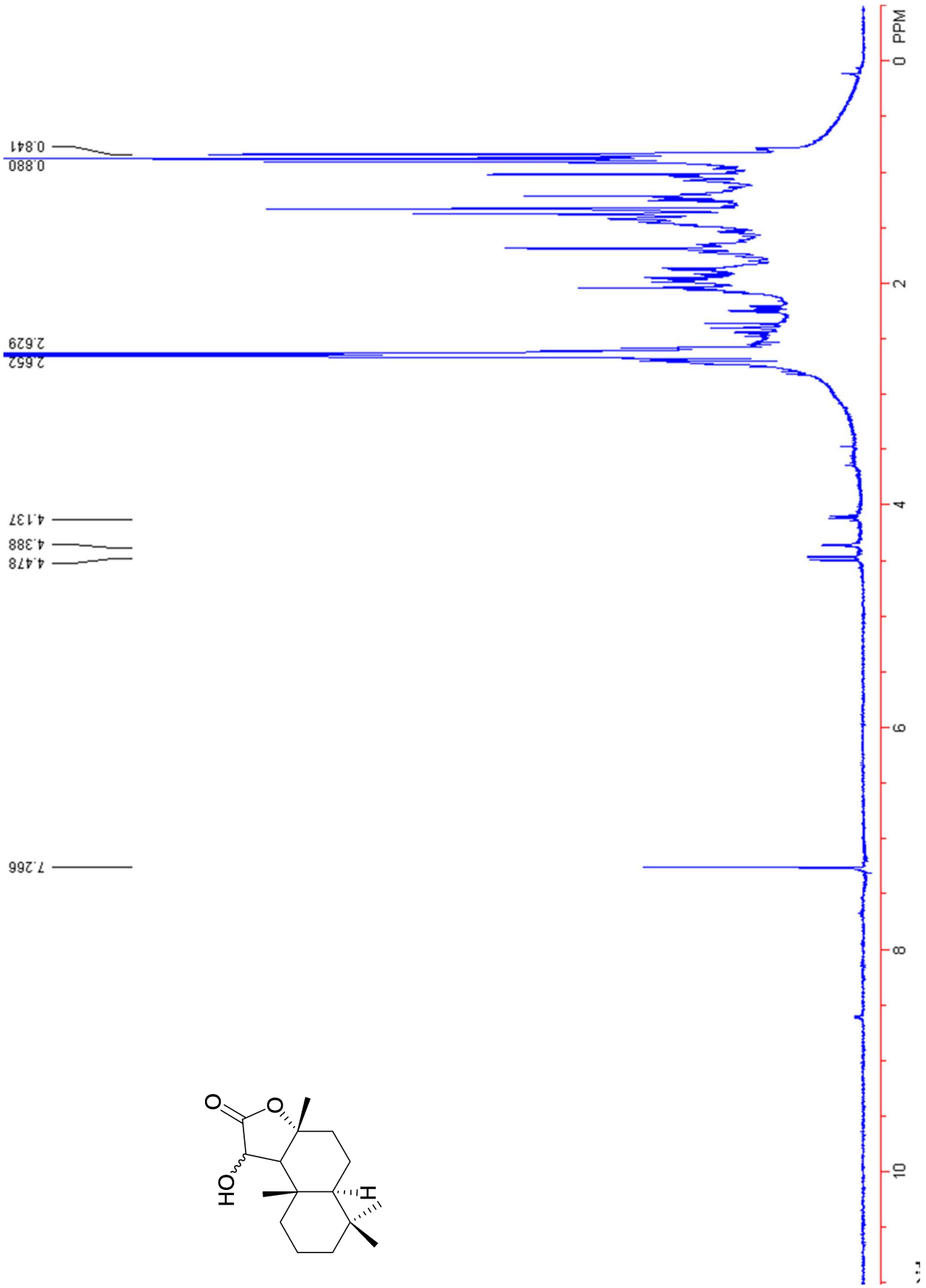
0.841
0.880
2.629
2.652
4.137
4.388
4.478
7.266
0 PPM
2
4
6
8
10
O
O
HO
H

1.214
1.221
1.230
1.234
1.248
1.266
1.280
1.285
1.297
1.325
1.340
1.385
1.400
2.035
1.413
1.418
1.426
1.439
1.466
1.481
1.492
1.504
1.506
1.511
1.524
1.570
1.576
1.586
1.590
1.596
1.601
1.606
1.632
1.639
1.652
1.660
1.670
1.749
1.755
1.784
7.253
0 PPM
2
4
6
8
10
OH
O
HO
H
+
OH
OH
HO
H

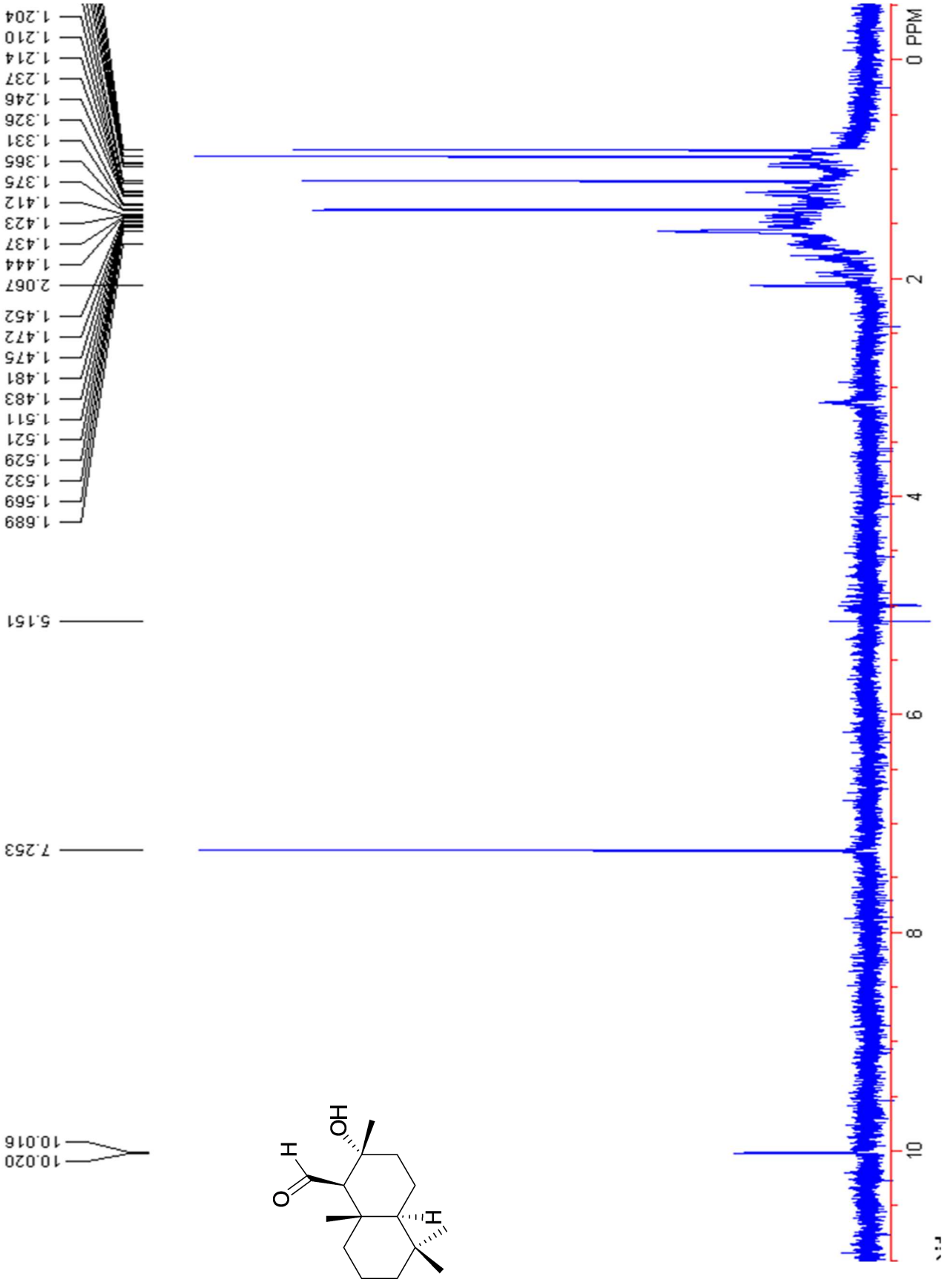
1.204
1.210
1.214
1.237
1.246
1.326
1.331
1.365
1.375
1.412
1.423
1.437
1.444
2.067
1.452
1.472
1.475
1.481
1.483
1.511
1.521
1.529
1.532
1.569
1.689
5.151
7.253
10.016
10.020
0 PPM
2
4
6
8
10
OH
H
O
H

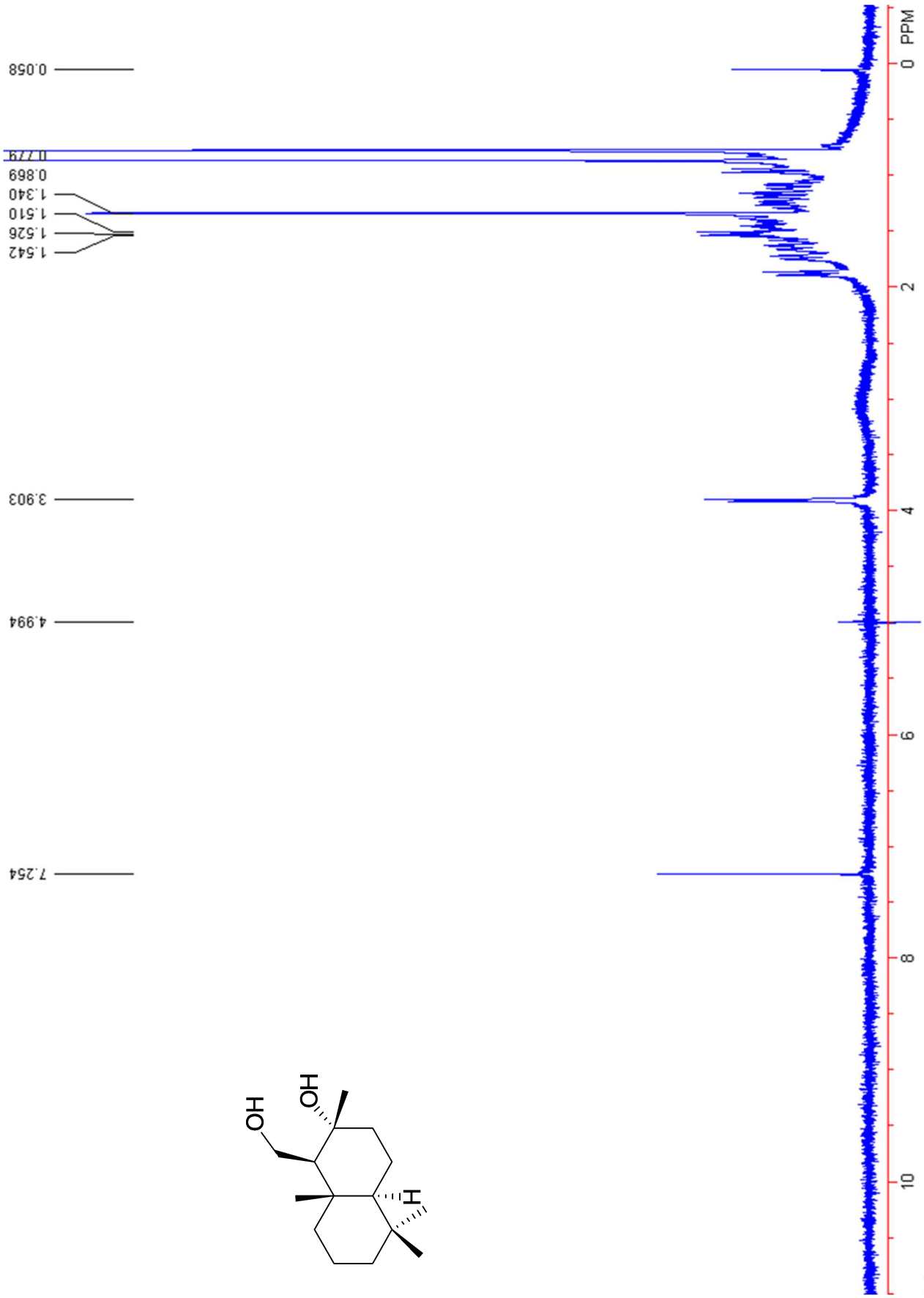
0.058
0.779
0.869
1.340
1.510
1.526
1.542
3.903
4.994
7.254
PPM
0
2
4
6
8
10
OH
OH
H

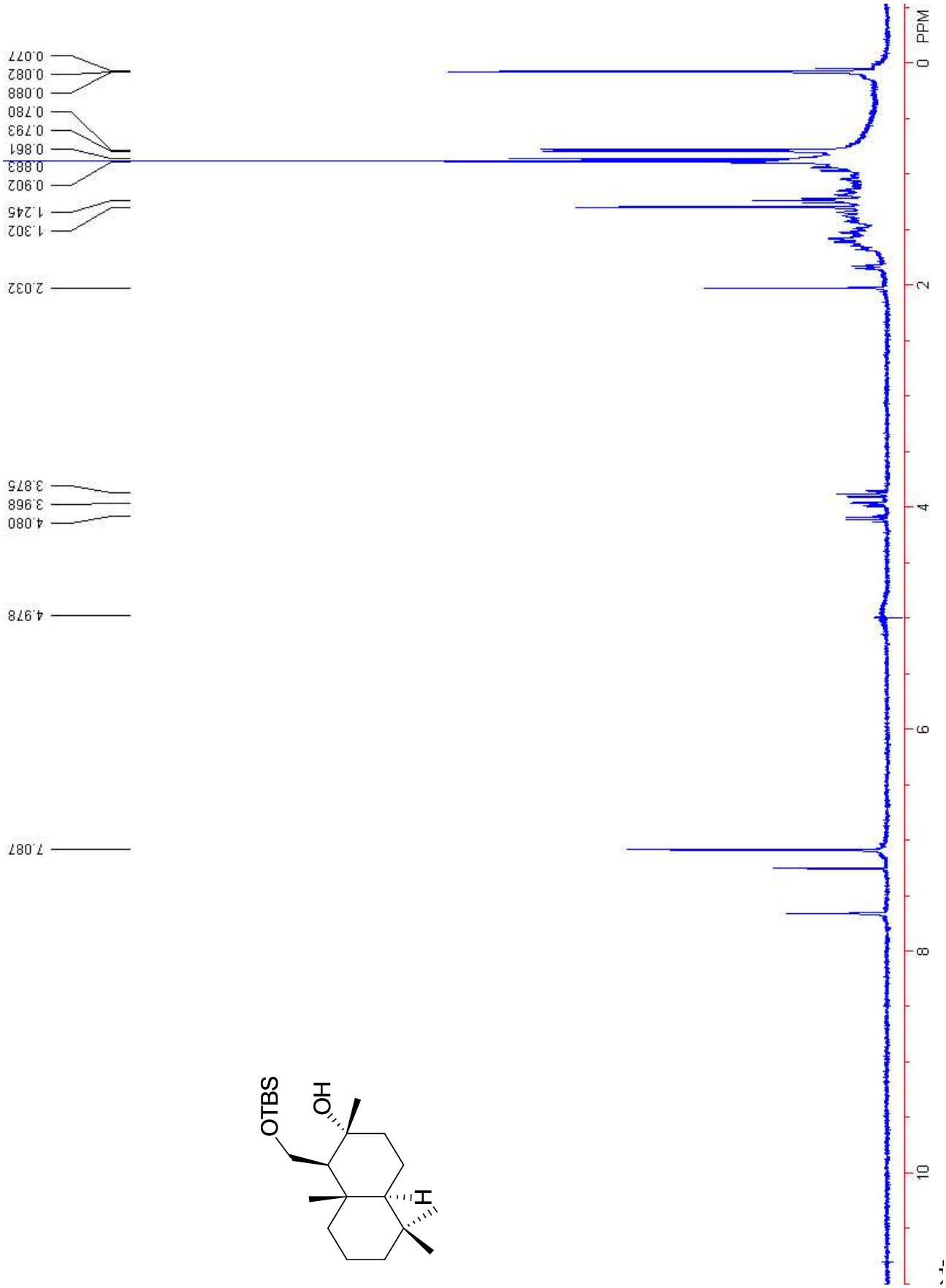
0.077
0.082
0.088
0.780
0.793
0.861
0.883
0.902
1.245
1.302
2.032
3.875
3.968
4.080
4.978
7.087
0 PPM
2
4
6
8
10
OTBS
OH
H

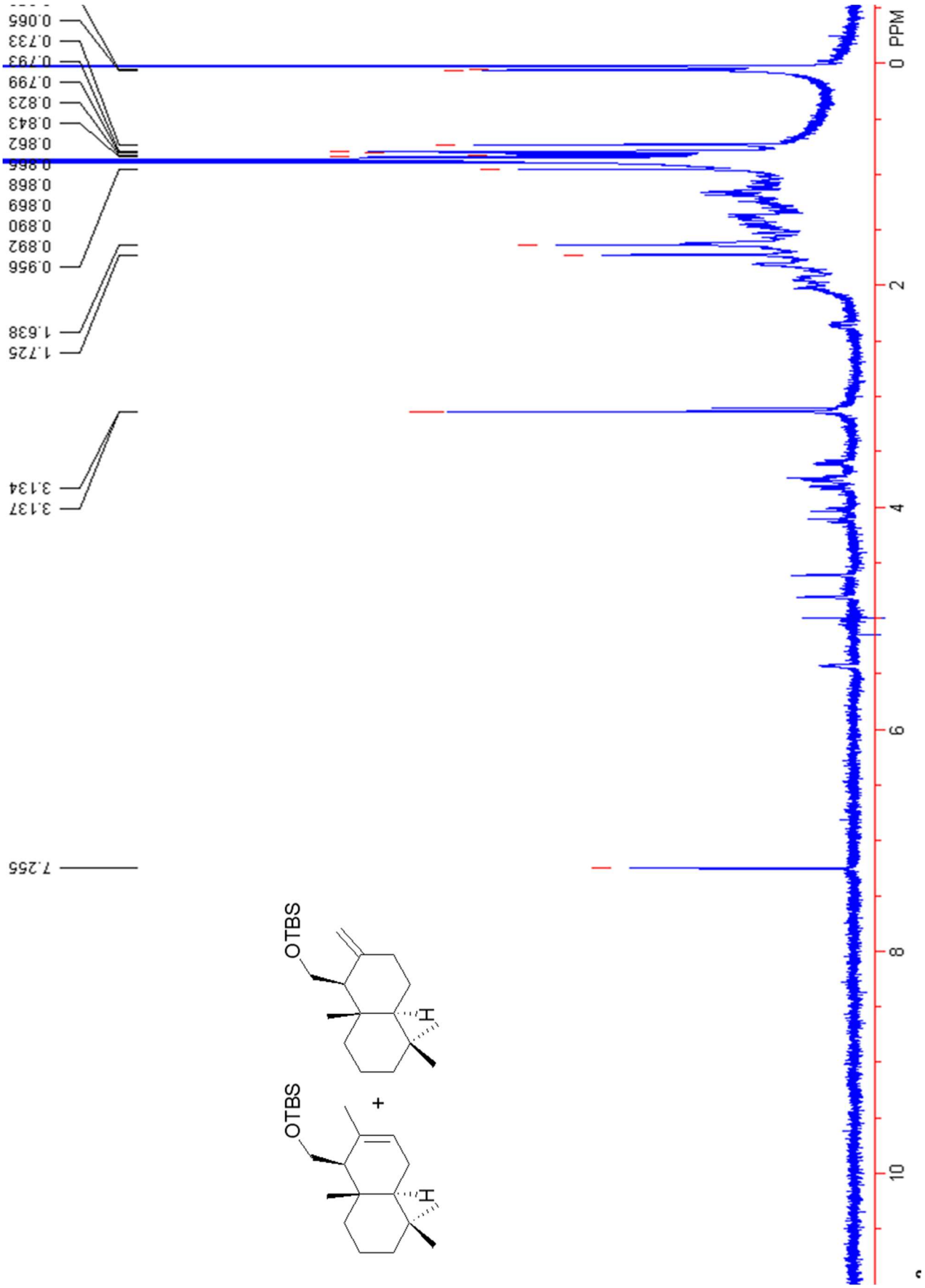
0.065
0.733
0.793
0.799
0.823
0.843
0.862
0.866
0.868
0.869
0.890
0.892
0.956
1.638
1.725
3.134
3.137
7.255
OTBS
H
+
OTBS
H
0 PPM
2
4
6
8
10

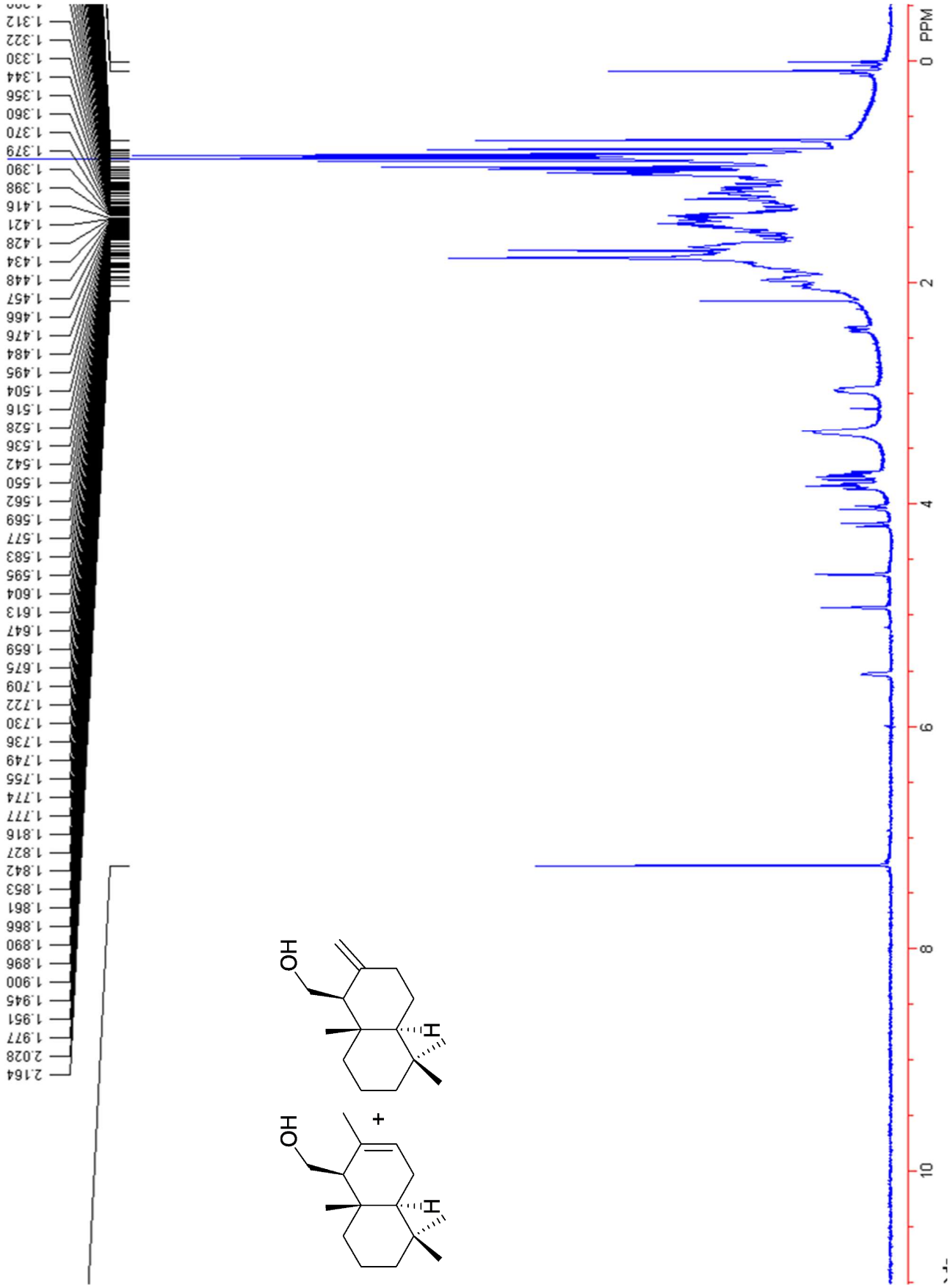
1.312
1.322
1.330
1.344
1.356
1.360
1.370
1.379
1.390
1.398
1.416
1.421
1.428
1.434
1.448
1.457
1.466
1.476
1.484
1.495
1.504
1.516
1.528
1.536
1.542
1.550
1.562
1.569
1.577
1.583
1.595
1.604
1.613
1.647
1.659
1.675
1.709
1.722
1.730
1.736
1.749
1.755
1.774
1.777
1.816
1.827
1.842
1.853
1.861
1.866
1.890
1.896
1.900
1.945
1.951
1.977
2.028
2.164
PPM
0
2
4
6
8
10
OH
H
+
OH
H

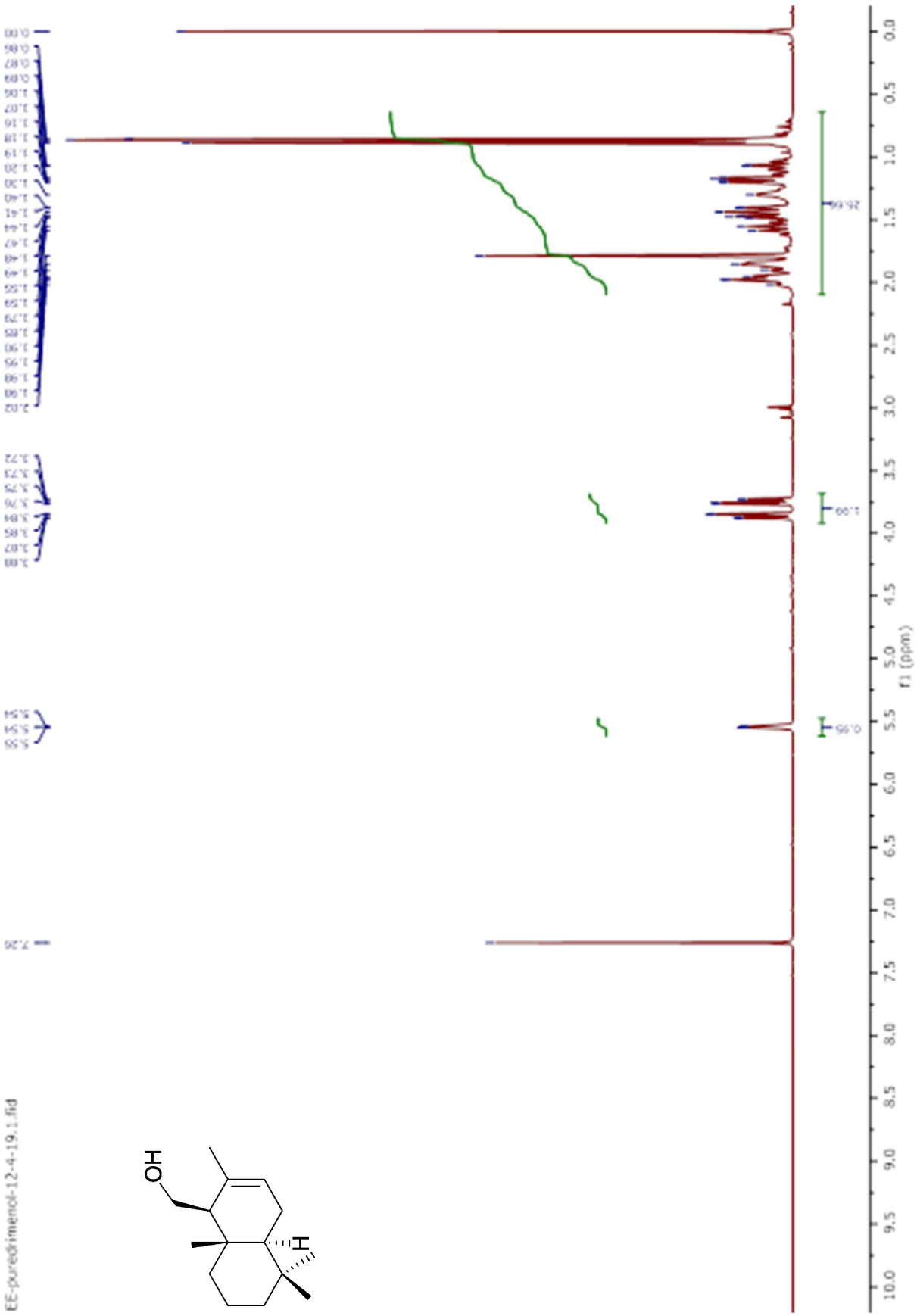
EE-puredrimenol-12-4-19.1.fid
f1 (ppm)

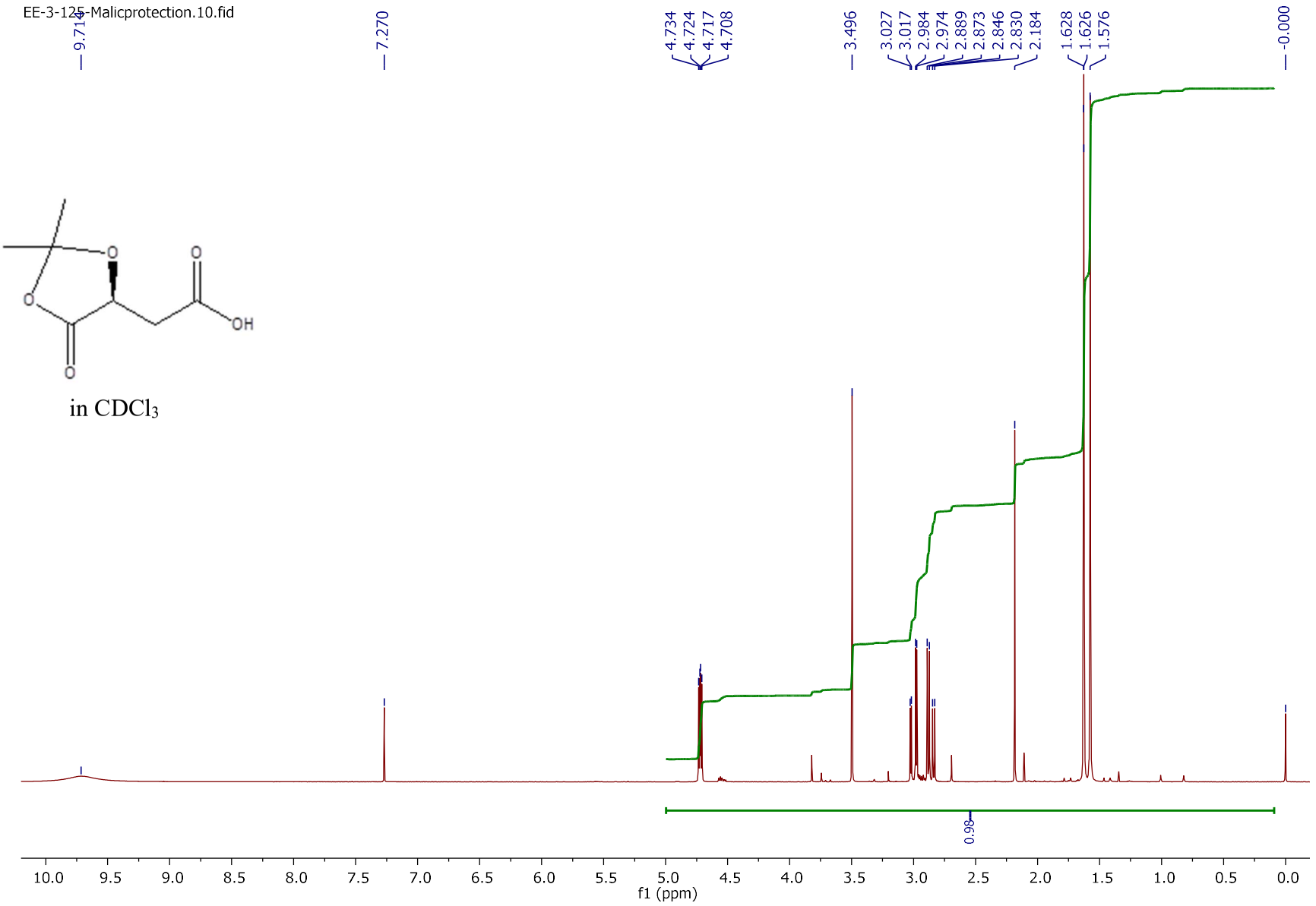
EE-3-125-Malicprotection.10.fid
9.714
7.270
4.734
4.724
4.717
4.708
3.496
3.027
3.017
2.984
2.974
2.889
2.873
2.846
2.830
2.184
1.628
1.626
1.576
-0.000
O
O
O
O
OH
in CDCl3
0.98
10.0
9.5
9.0
8.5
8.0
7.5
7.0
6.5
6.0
5.5
5.0
4.5
4.0
3.5
3.0
2.5
2.0
1.5
1.0
0.5
0.0
f1 (ppm)

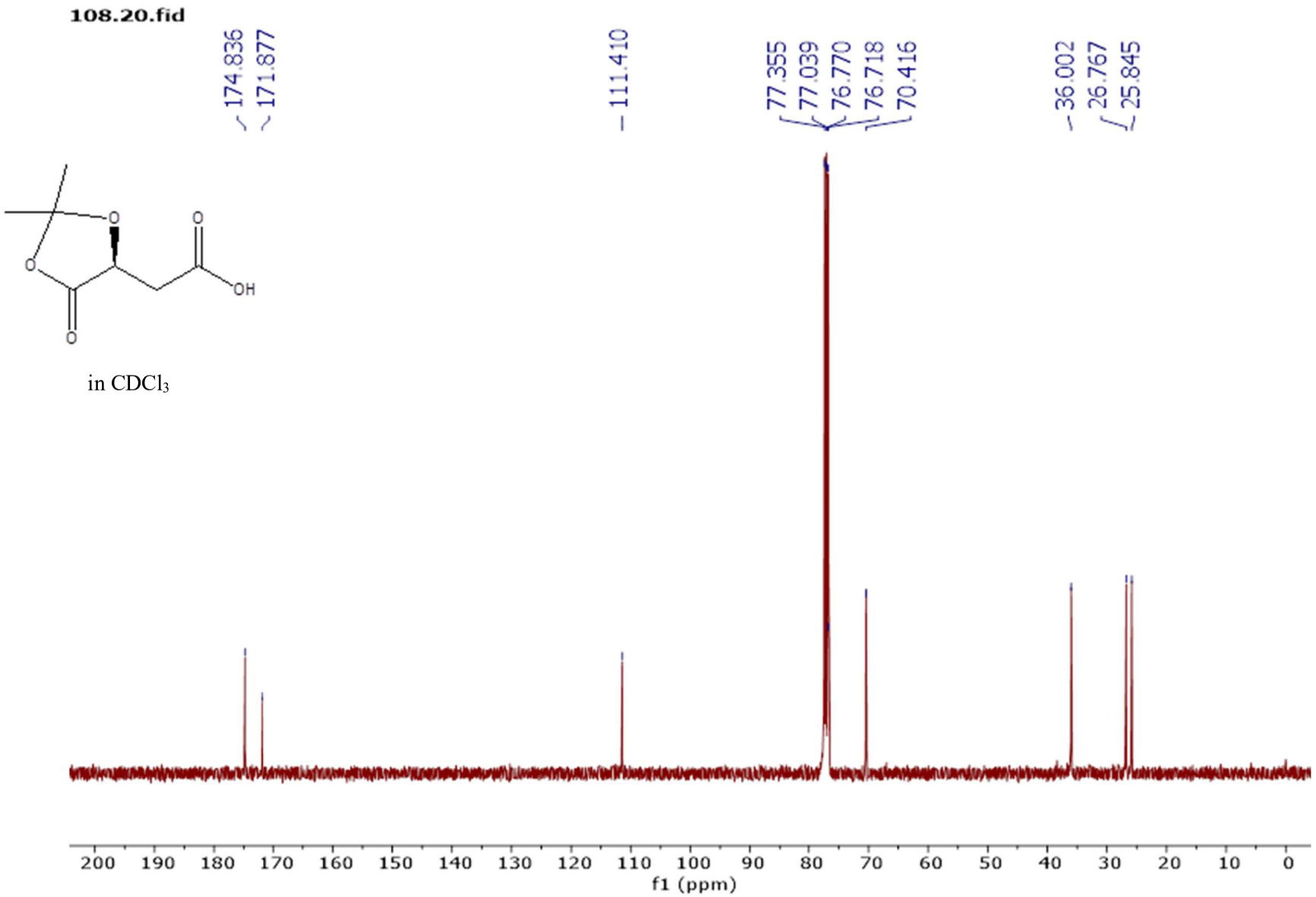
108.20.fid
174.836
171.877
111.410
77.355
77.039
76.770
76.718
70.416
36.002
26.767
25.845
O
O
O
O
OH
200 190 180 170 160 150 140 130 120 110 100 90 80 70 60 50 40 30 20 10 0
f1 (ppm)

in $CDCl_3$

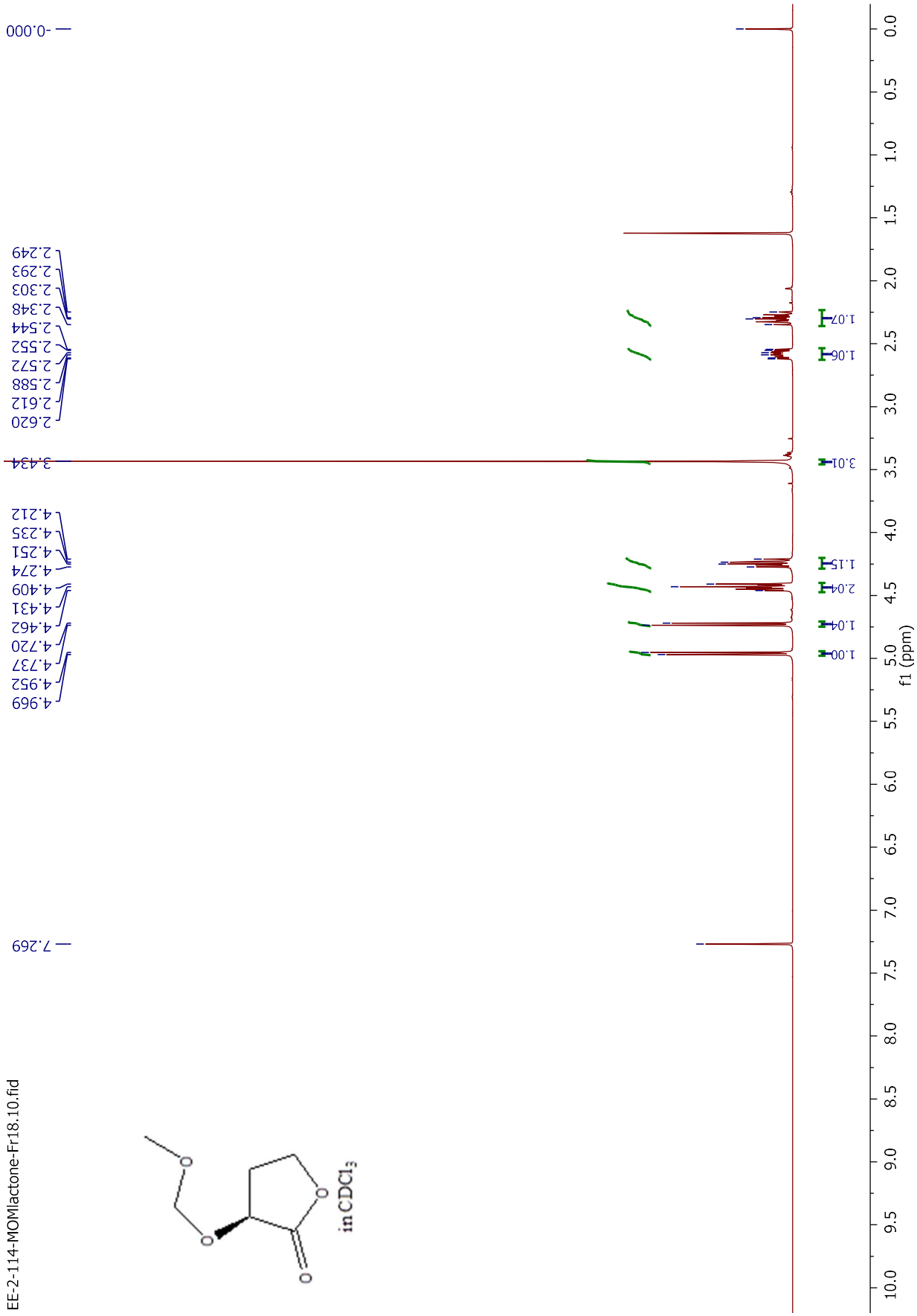
EE-2-114-MOMlactone-Fr18.10.fid
in CDCl3
-0.000
7.269
4.969
4.952
4.737
4.720
4.462
4.431
4.409
4.274
4.251
4.235
4.212
3.434
2.620
2.612
2.588
2.572
2.552
2.544
2.348
2.303
2.293
2.249
1.00
1.04
2.04
1.15
3.01
1.06
1.07
f1 (ppm)

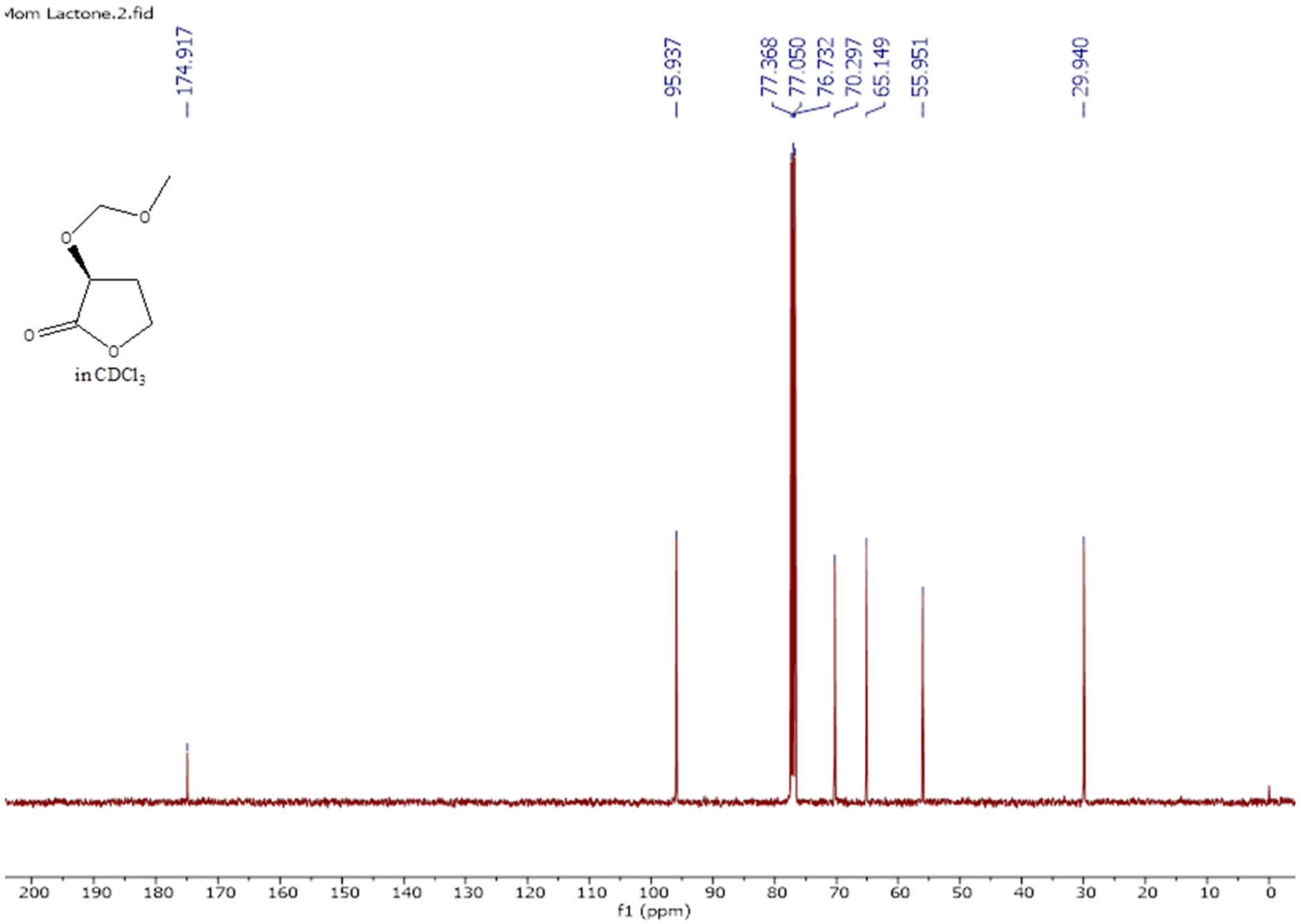
Mom Lactone.2.fid
174.917
95.937
77.368
77.050
76.732
70.297
65.149
55.951
29.940
O
O
O
O
in $CDCl_3$
200 190 180 170 160 150 140 130 120 110 100 90 80 70 60 50 40 30 20 10 0
f1 (ppm)

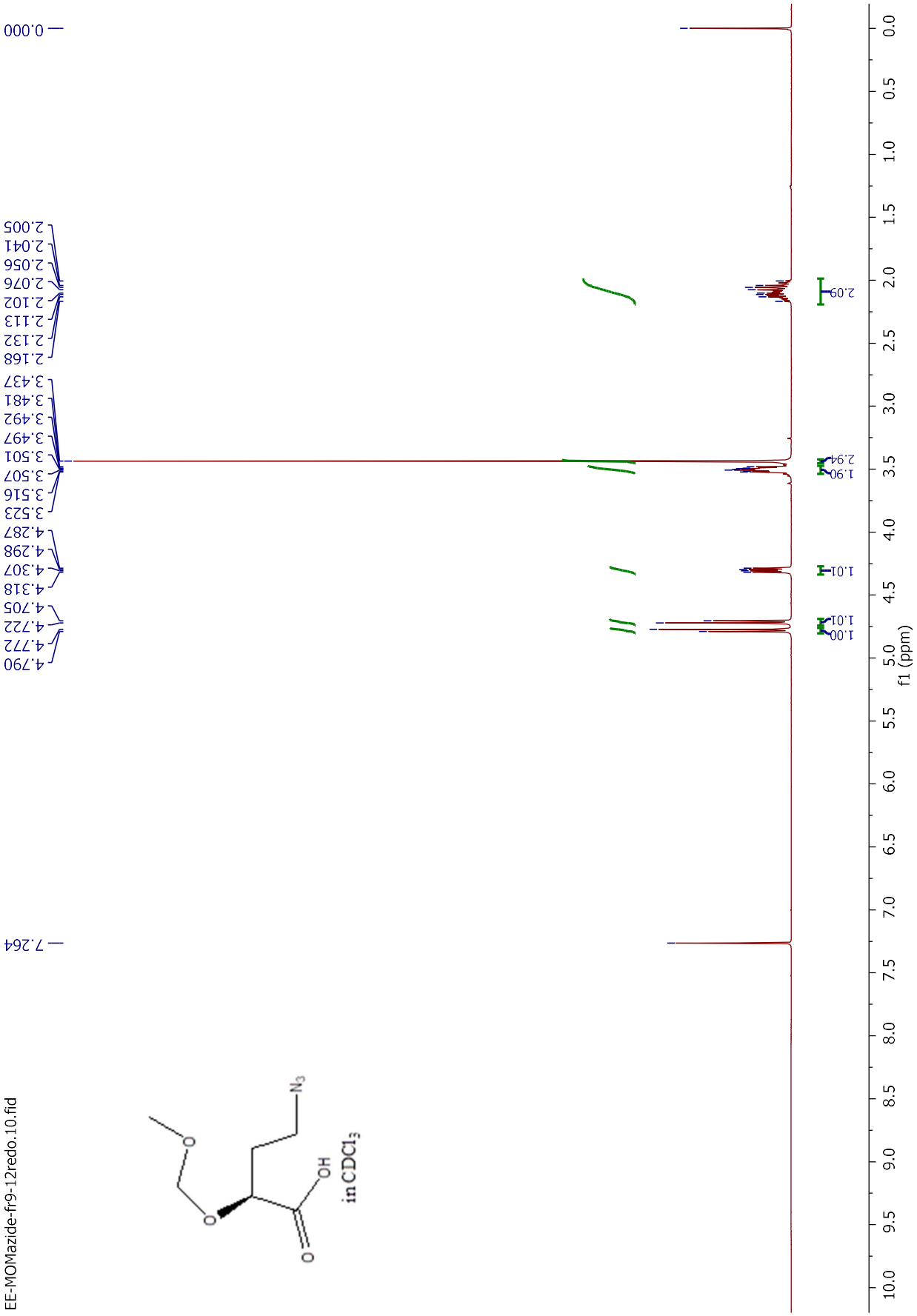
EE-MOMazide-fr9-12redo.10.fid
in $CDCl_3$
f1 (ppm)
0.000
7.264
4.790
4.772
4.722
4.705
4.318
4.307
4.298
4.287
3.523
3.516
3.507
3.501
3.497
3.492
3.481
3.437
2.168
2.132
2.113
2.102
2.076
2.056
2.041
2.005
2.09
1.90
2.94
1.01
1.00
1.01

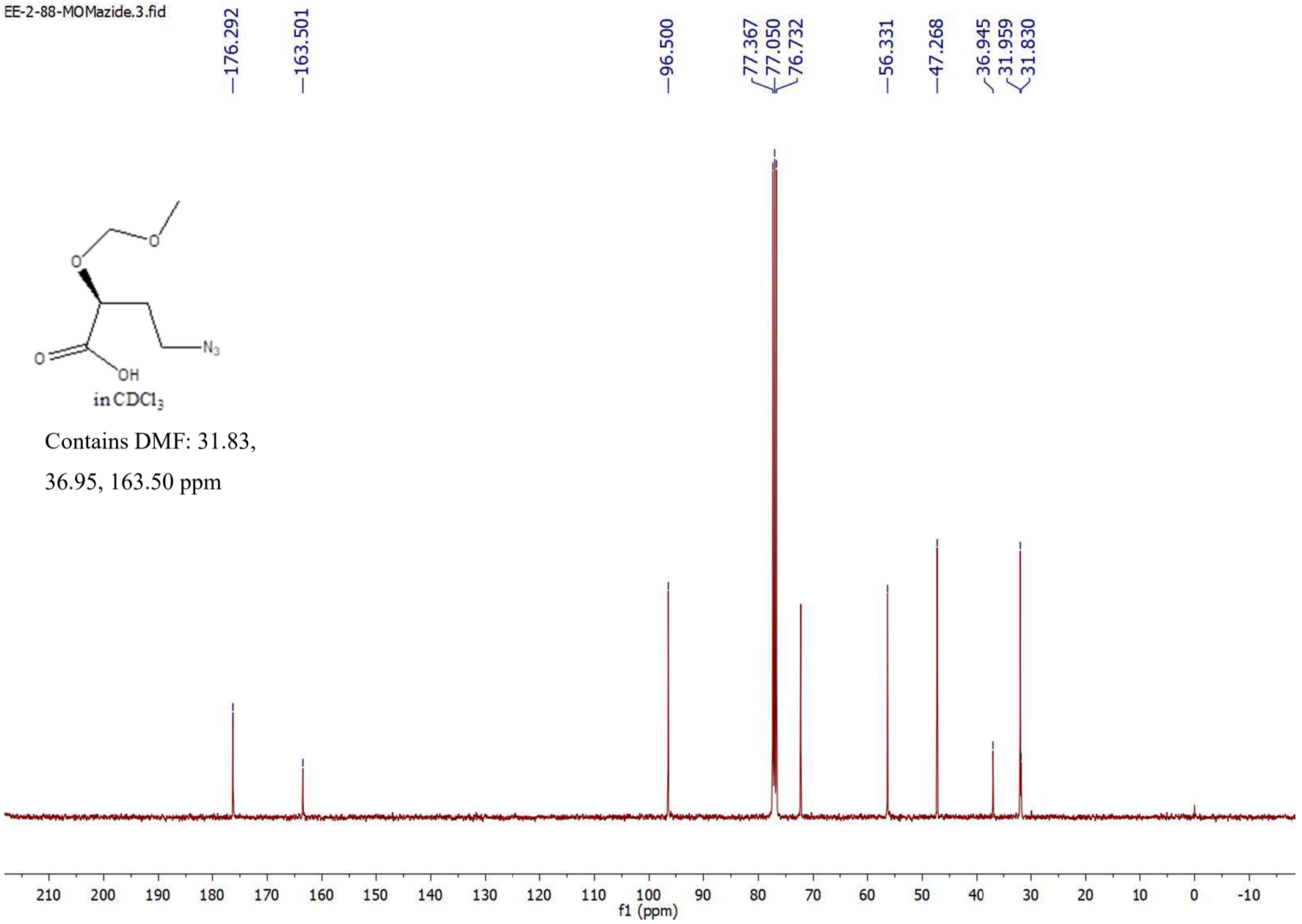

Contains DMF: 31.83, 36.95, 163.50 ppm

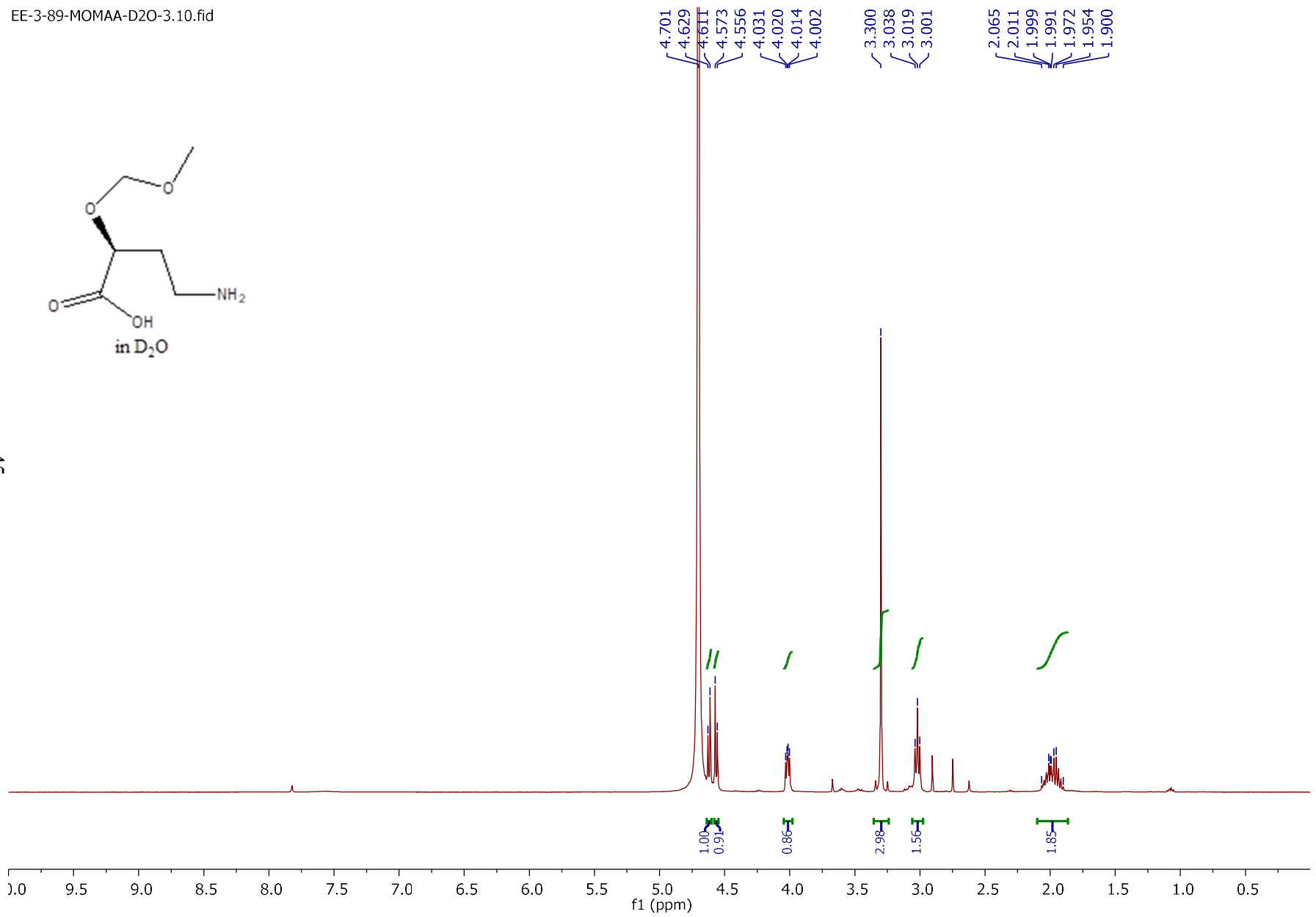
EE-3-89-MOMAA-D2O-3.10.fid
4.701
4.629
4.611
4.573
4.556
4.031
4.020
4.014
4.002
3.300
3.038
3.019
3.001
2.065
2.011
1.999
1.991
1.972
1.954
1.900
O
O
O
NH2
OH
in D2O
1.00
0.91
0.86
2.98
1.56
1.85
f1 (ppm)

EE-3-89-MOMAA-D2O-3.11.fid

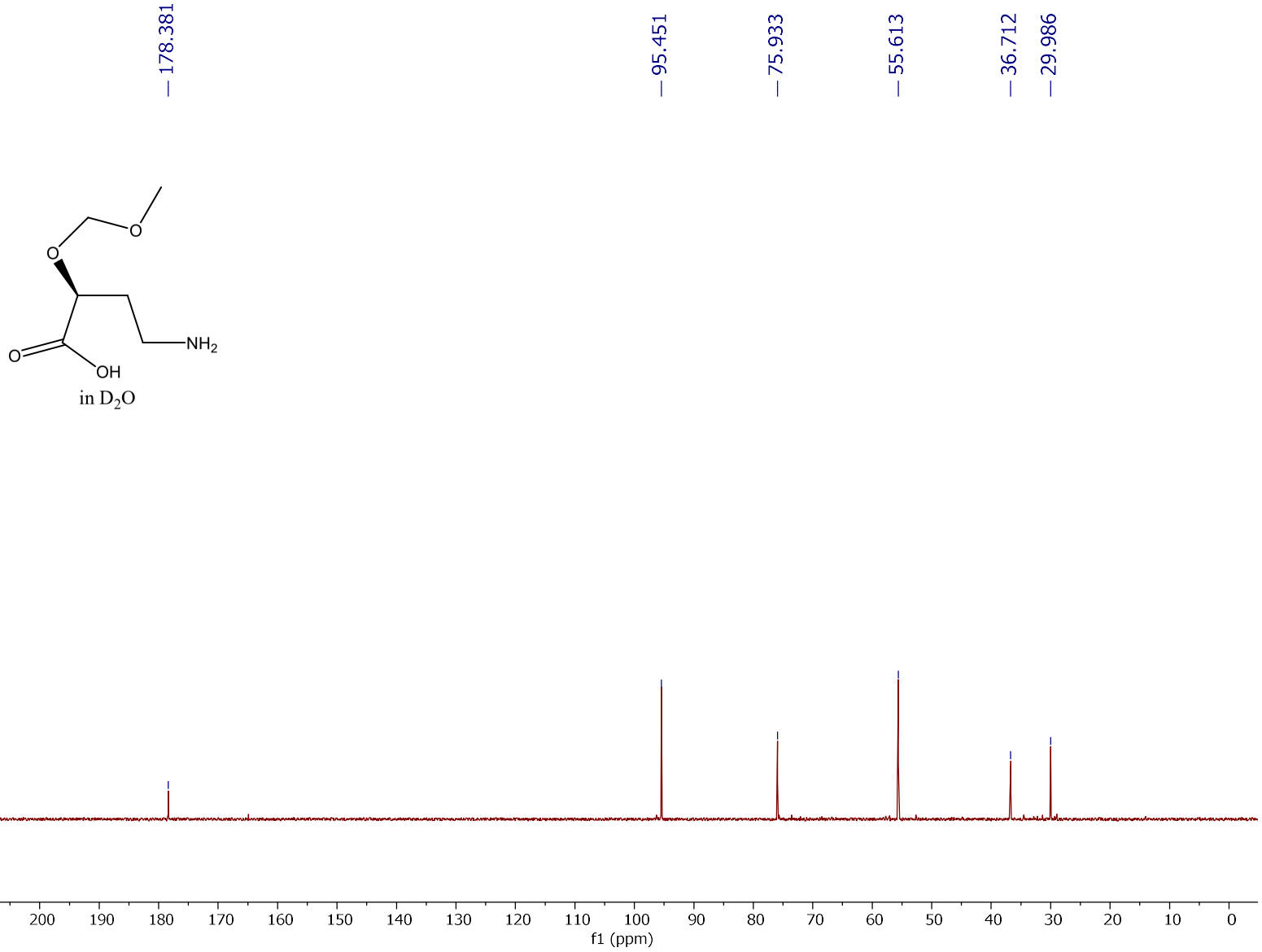

EE-2-100-MOMlactam.1.fid

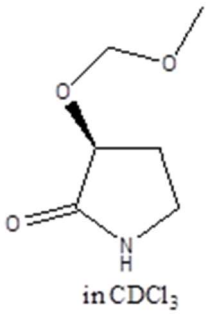

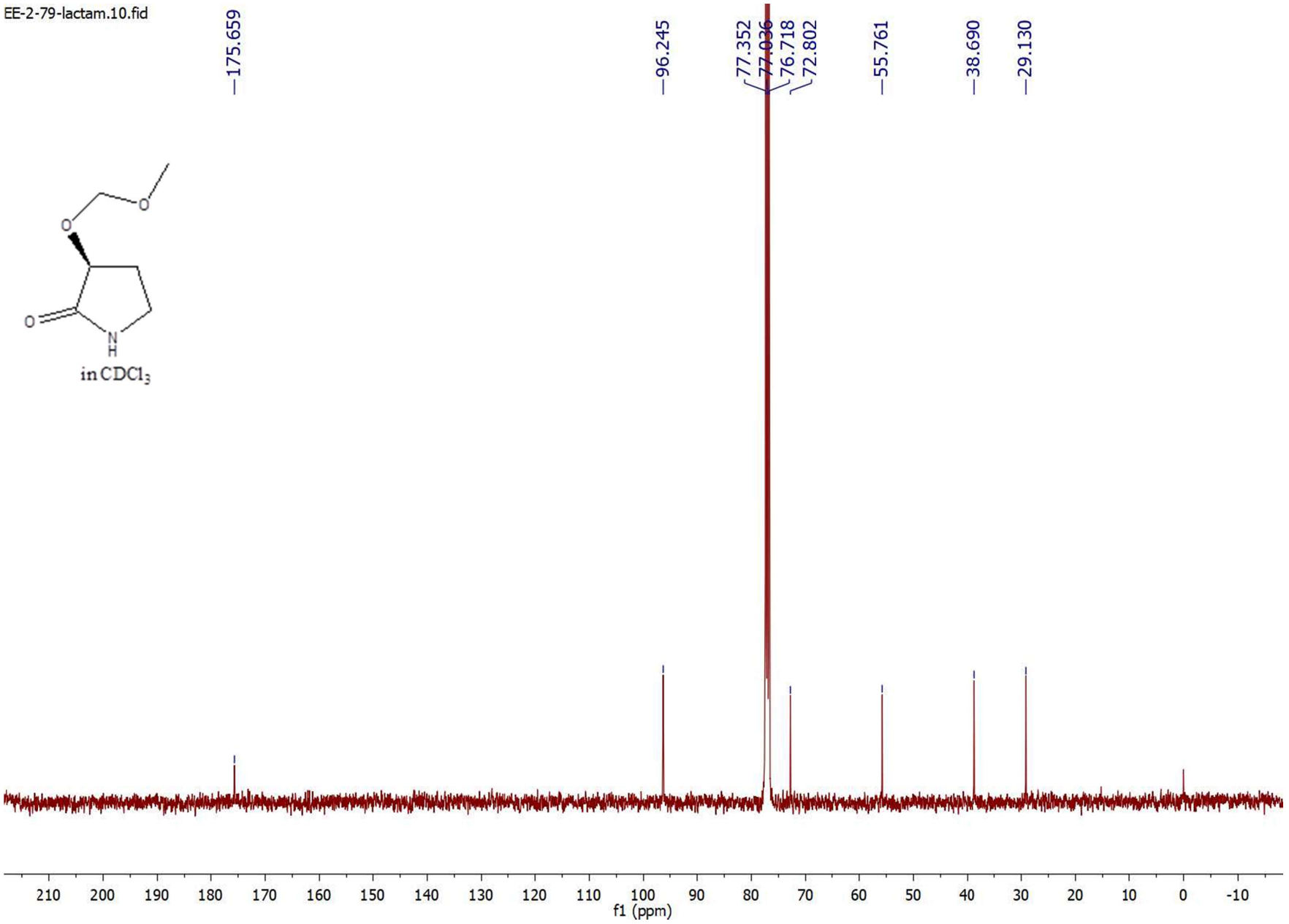
EE-2-79-lactam.10.fid
175.659
96.245
77.352
77.036
76.718
72.802
55.761
38.690
29.130
O
O
O
N
H
in CDCl3
210
200
190
180
170
160
150
140
130
120
110
100
90
80
70
60
50
40
30
20
10
0
-10
f1 (ppm)

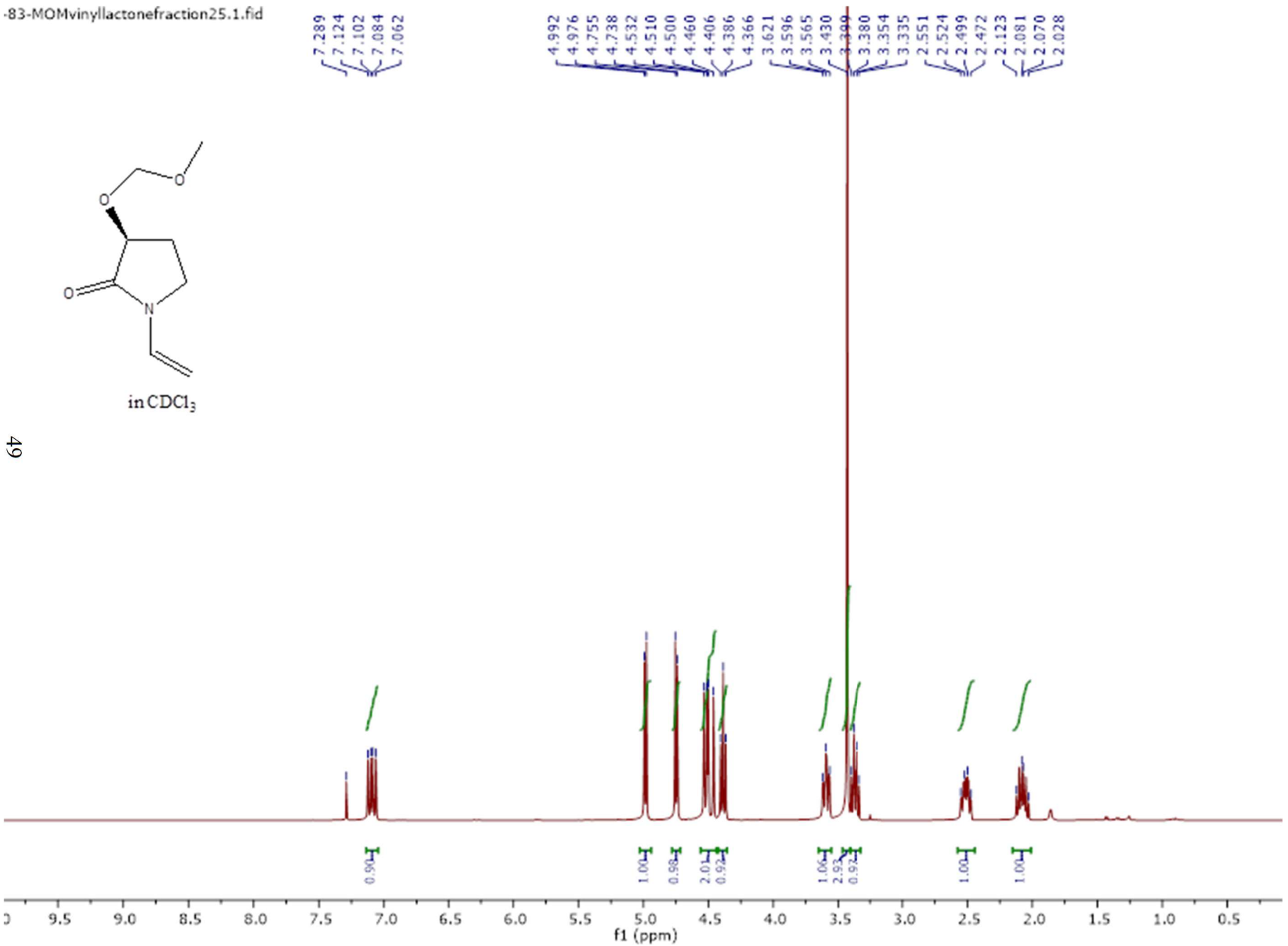
-83-MOMvinyllactonefraction25.1.fid
7.289
7.124
7.102
7.084
7.062
4.992
4.976
4.755
4.738
4.532
4.510
4.500
4.460
4.406
4.386
4.366
3.621
3.596
3.565
3.430
3.399
3.380
3.354
3.335
2.551
2.524
2.499
2.472
2.123
2.081
2.070
2.028
O
O
O
N
in $CDCl_3$
0.90
1.00
0.98
2.01
0.92
1.00
2.93
0.97
1.00
1.00
f1 (ppm)

EE-2-83-MOMvinyllactonefraction25.2.fid

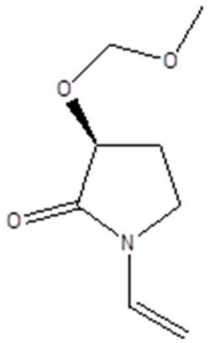

in $CDCl_3$

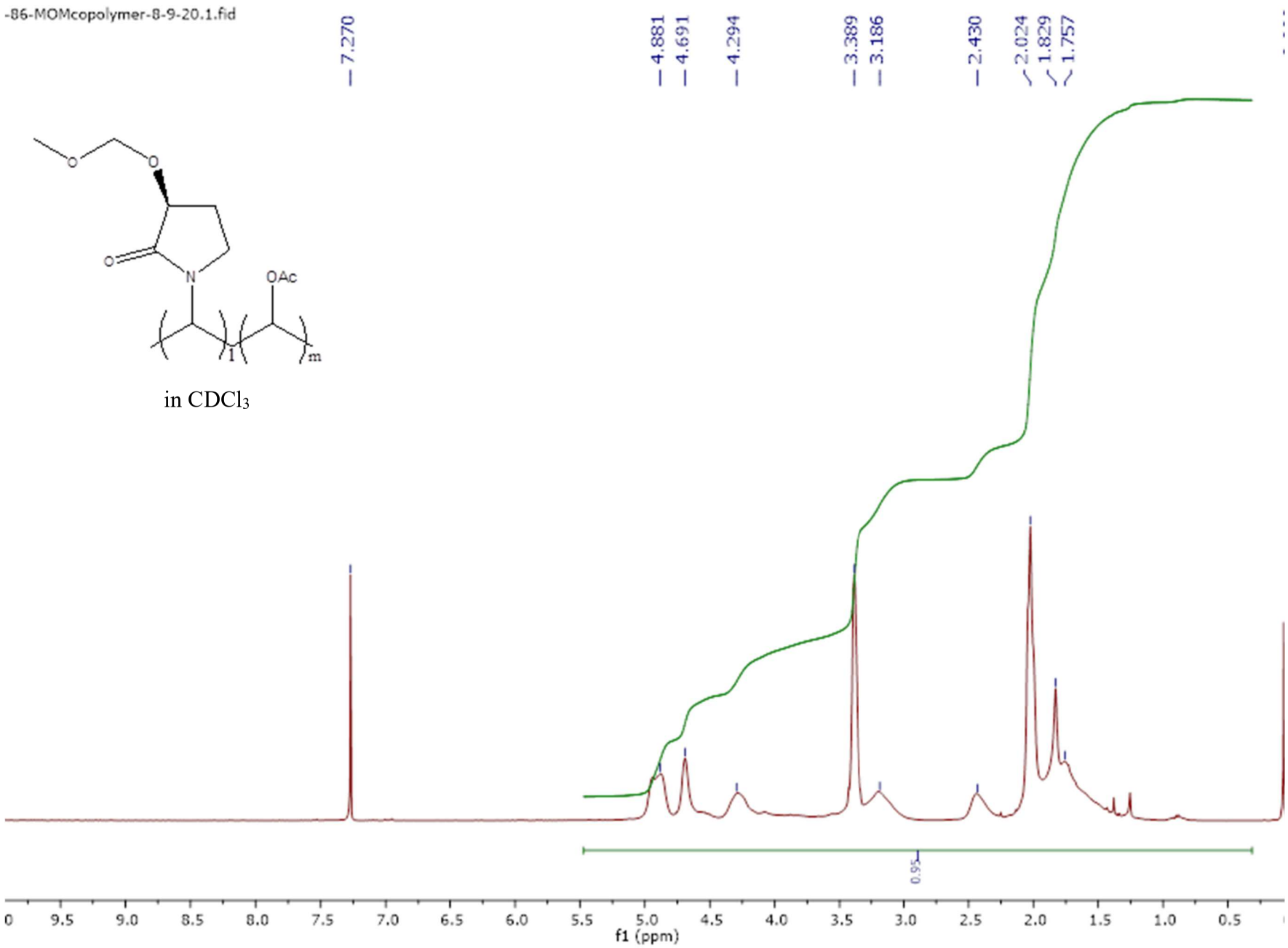
-86-MOMcopolymer-8-9-20.1.fid
7.270
4.881
4.691
4.294
3.389
3.186
2.430
2.024
1.829
1.757
O
O
O
N
OAc
l
m
0.95
f1 (ppm)

in $CDCl_3$

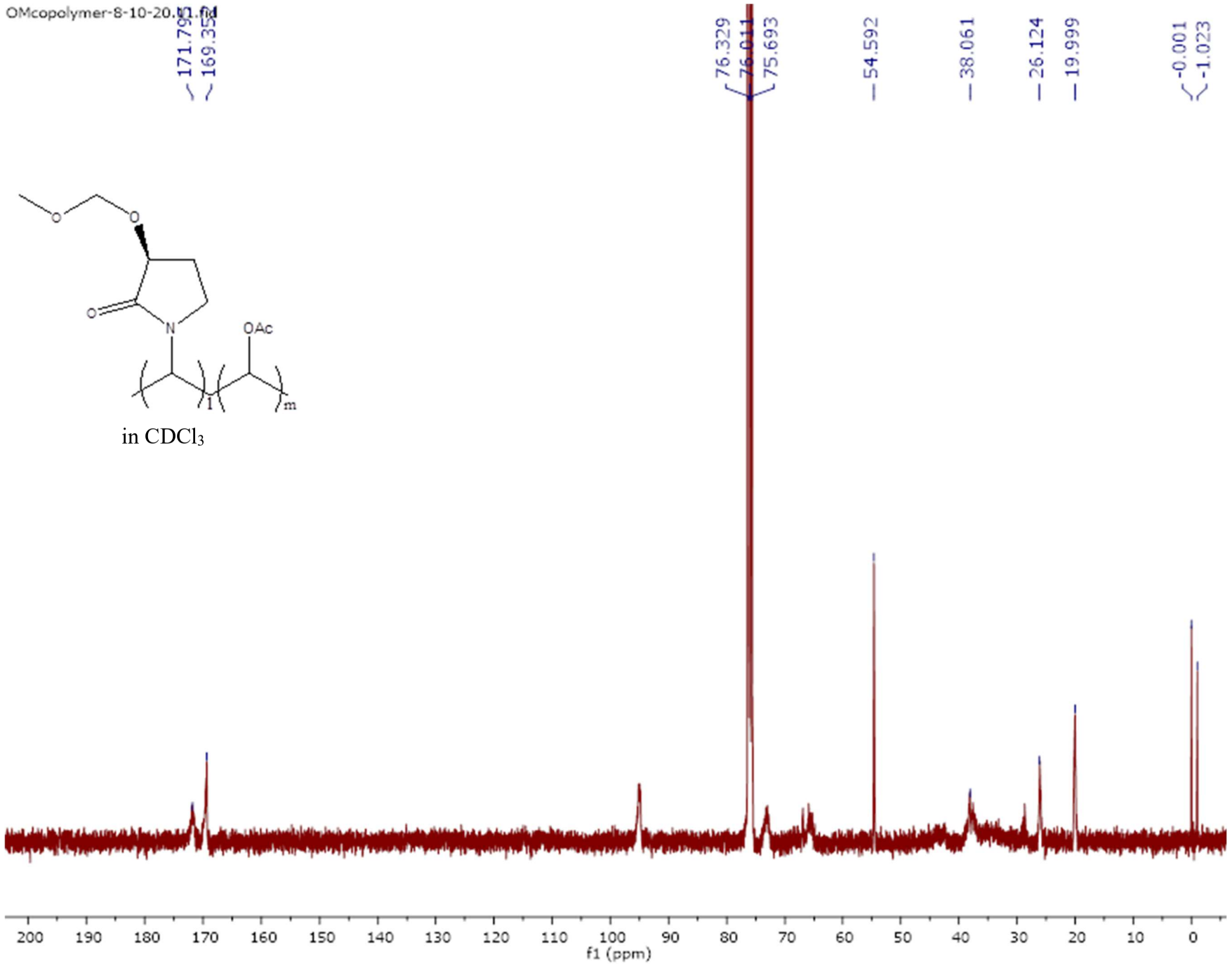
OMcopolymer-8-10-20.11.fid
171.795
169.354
76.329
76.011
75.693
54.592
38.061
26.124
19.999
-0.001
-1.023
O
O
O
N
OAc
l
m
200
190
180
170
160
150
140
130
120
110
100
90
80
70
60
50
40
30
20
10
0
f1 (ppm)

in $CDCl_3$

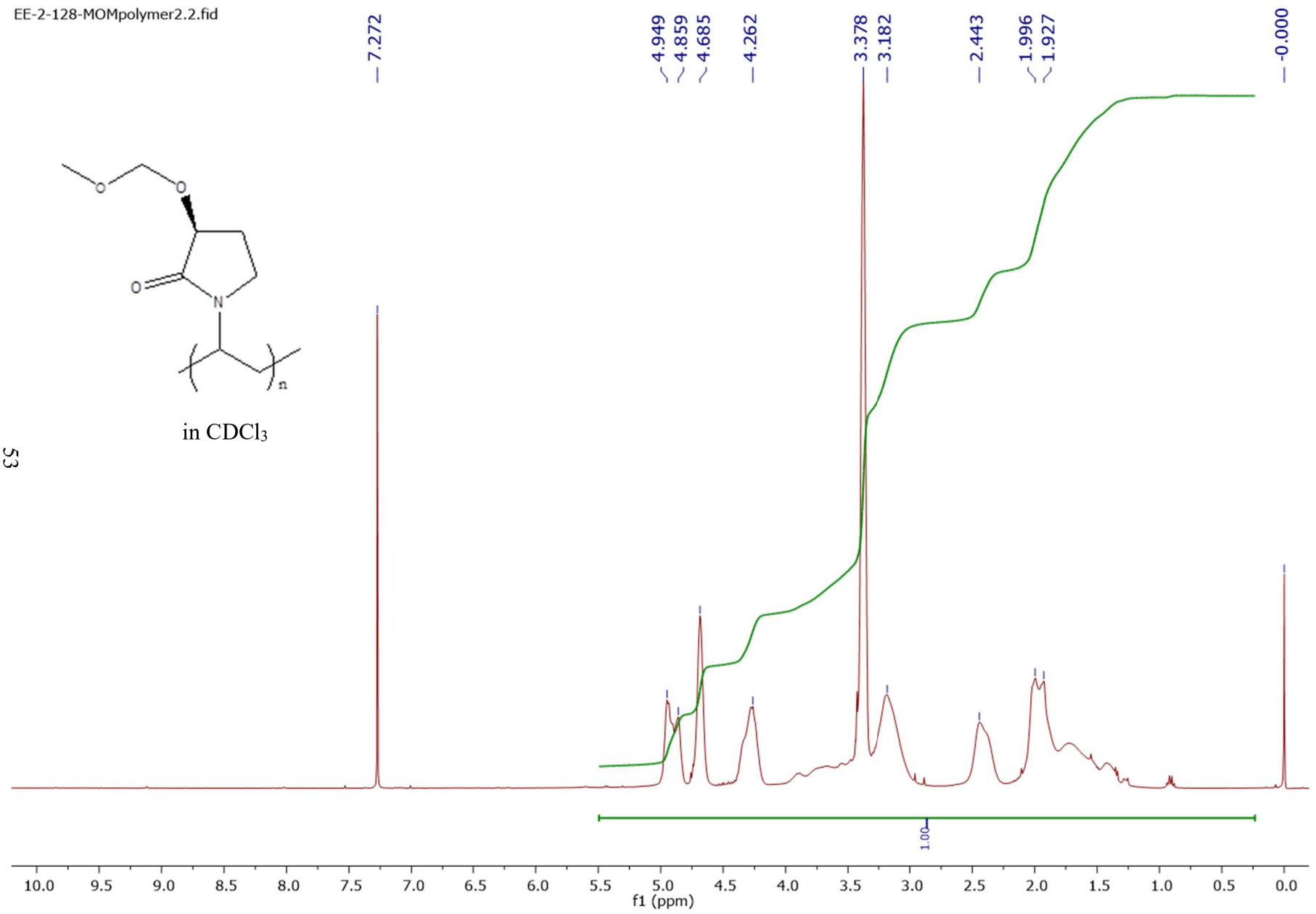
EE-2-128-MOMpolymer2.2.fid
7.272
4.949
4.859
4.685
4.262
3.378
3.182
2.443
1.996
1.927
-0.000
O
O
O
N
n
in CDCl3
1.00
10.0
9.5
9.0
8.5
8.0
7.5
7.0
6.5
6.0
5.5
5.0
4.5
4.0
3.5
3.0
2.5
2.0
1.5
1.0
0.5
0.0
f1 (ppm)

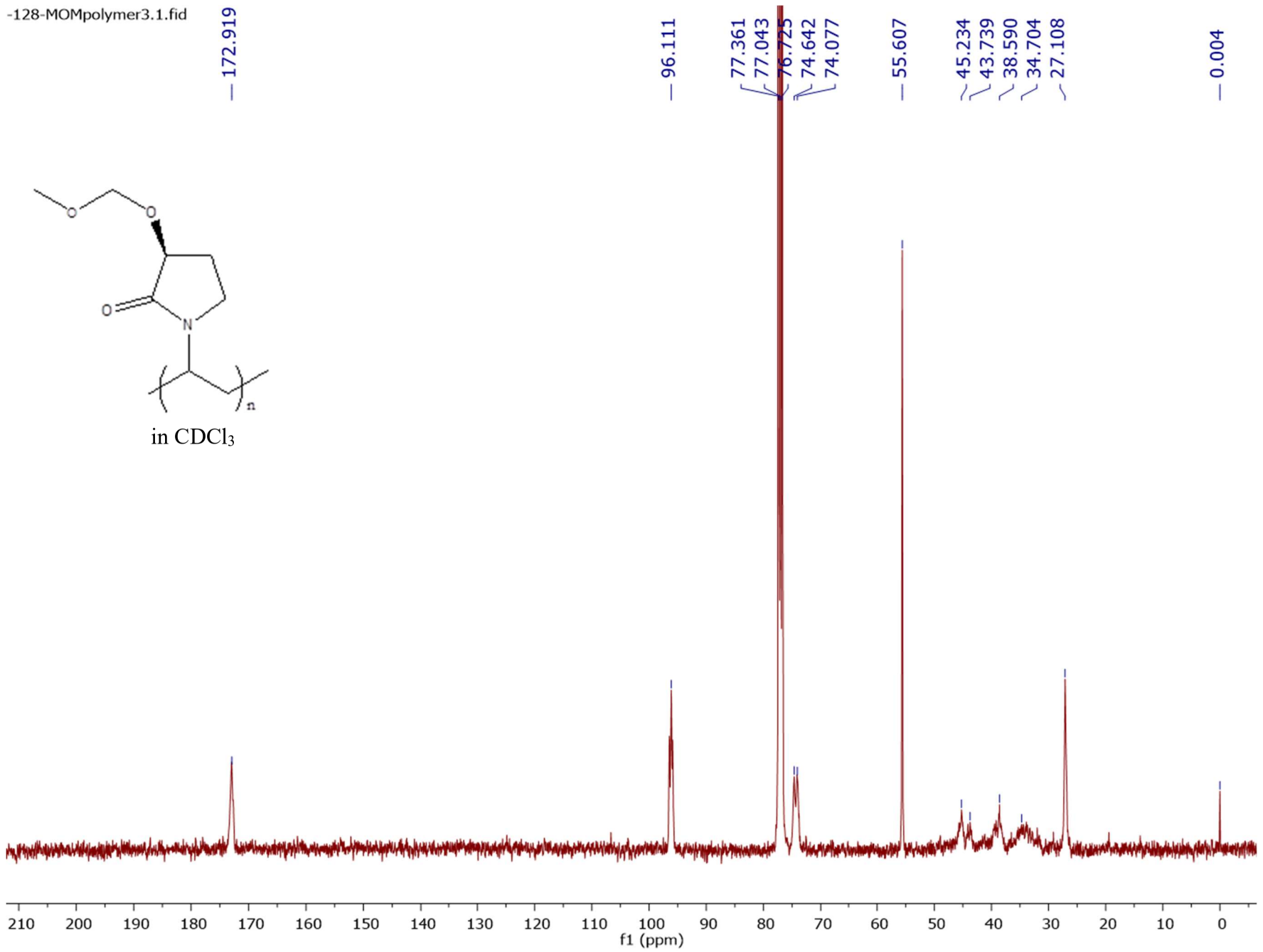
-128-MOMpolymer3.1.fid
172.919
96.111
77.361
77.043
76.725
74.642
74.077
55.607
45.234
43.739
38.590
34.704
27.108
0.004
O
O
O
N
n
in CDCl3
210 200 190 180 170 160 150 140 130 120 110 100 90 80 70 60 50 40 30 20 10 0
f1 (ppm)